Lithology and Mineral Resources, Vol. 40, No. 4, 2005, pp. 293–319. Translated from Litologiya i Poleznye Iskopaemye, No. 4, 2005, pp. 339–367.

Mineral Assemblages as Indicators of the Maturity of Oceanic Hydrothermal Sulfide Mounds

N. N. Mozgova[1], Yu. S. Borodaev[2], I. F. Gablina[3], G. A. Cherkashev[4], and T. V. Stepanova[4]

[1] *Institute of Geology of Ore Deposits, Petrography, Mineralogy, and Geochemistry, Russian Academy of Sciences, Staromonetnyi per. 35, Moscow, 119017 Russia*
e-mail: mozgova@igem.ru
[2] *Department of Economic Geology, Geological Faculty, Moscow State University, Vorob'evy gory, Moscow, 119992 Russia*
[3] *Geological Institute, Russian Academy of Sciences, Pyzhevskii per. 7, Moscow, 119017 Russia*
[4] *All-Russia Research Institute of Geology and Mineral Resources of the World Ocean (VNIIOkeanologiya), Angliiskii pr. 1, St. Petersburg, 190121 Russia*

Received September 27, 2004

Abstract—The composition of ore minerals in MAR sulfide occurrences related to ultramafic rocks was studied using methods of mineragraphy, electron microscopy, microprobe analysis, and X-ray analysis. The objects are located at various levels of the maturity of sulfide mounds owing to differences in age, duration, and degree of activity of the following hydrothermal systems: generally inactive Logatchev-1 field (up to 66.5 ka old), inactive Logatchev-2 field (3.9 ka), and generally active Rainbow field (up to 23 ka). Relative to MAR submarine ore occurrences in the basalt substrate, mineralization in the hydrothermal fields mentioned above is characterized by high contents of Au, Cd, Co, and Ni, along with the presence of accessory minerals of Co and Ni. The studied mounds differ in quantitative ratios of major minerals and structural–textural features of ores that suggest their transformation. Ores in the Logatchev-1 field are characterized by the highest Cu content and the development of a wide range of multistage contrast exsolution structures of isocubanite and bornite. In the Logatchev-2 field, sphalerite–chalcopyrite and gold–arsenic exsolution structures are present, but isocubanite exsolution structures are less diverse and contrast. The Rainbow field is marked by the presence of homogenous isocubanite and the subordinate development of exsolution structures. We have identified four new phases in the Cu–Fe–S system. Phases X and Y (close to chalcopyrite and isocubanite, respectively) make up lamellae among isocubanite exsolution products in Logatchev-1 and Logatchev-2. Phase Y includes homogenous zones in zonal chimneys of the Rainbow field. Phases A and B are formed in the orange bornite domain at low-temperature alteration of chalcopyrite in the Logatchev-1 field. Mineral assemblages of the Cu–S system are most abundant and diverse in the Logatchev-1 field, but their development is minimal in the Logatchev-2 field where mainly Cu-poor sulfides of the geerite–covellite series have been identified. Specific features of mineral assemblages mentioned above reflect the maturity grade of sulfide mounds and can serve as indicators of maturity.

INTRODUCTION

Hydrothermal ore fields Logatchev-1, initially called Polyarnoe (Lazareva *et al.*, 1981), Logatchev-2, and Rainbow, which were discovered in the internal rift of the Mid-Atlantic Ridge in the latest ten years (Fig. 1), have received much attention, primarily, owing to their association with ultramafic rocks, in contrast to the more widespread hydrothermal formations associated with oceanic basalts. Based on several specific features, these hydrothermal fields have been referred to as a new type of modern hydrothermal systems (Bogdanov, 1997; Bogdanov *et al.*, 1997; 2000).

The geological setting and general characteristics of hydrothermal fields have been described in (Bogdanov, 1997; Bogdanov and Sagalevich, 2002; Bogdanov *et al.*, 1997, 2000, 2002; Fouquet *et al.*, 1998; Lazareva *et al.*, 1998; Lein *et al.*, 2001, 2003; Mozgova *et al.*, 1999; Rona *et al.*, 1987; Vikent'ev, 2001; and others). Therefore, only the main characteristics are given in the present communication (Table 1). All fields are sufficiently large and located on tectonic scarps of rift valley slopes at a depth of 2270 to 3040 m. The Logatchev-1 and Rainbow fields are located at the maximal and minimal depths, respectively. Relative to submarine ores on basalt substrates, these ore occurrences are characterized by higher Au, Cd, Co, Ni contents. At the same time, they differ from each other in the intensity of hydrothermal activity and age. The Logatchev-1 field (up to 66.5 ka old) is generally inactive (only some active sectors are preserved). The hydrothermal activity has completely terminated in the Logatchev-2 field (3.9 ka). The Rainbow field (up to 23 ka old) is generally active (more than 12 large active vents have been recorded here). The eastern sector of the Rainbow field (smoke zone) incorporates the youngest active black

0024-4902/05/4004-0293 © 2005 MAIK "Nauka/Interperiodica"

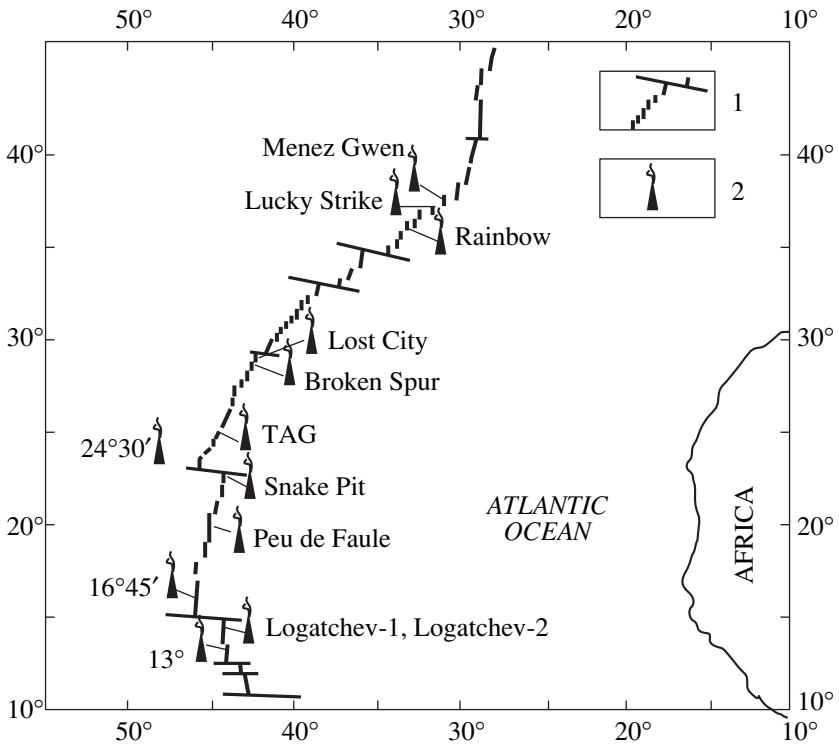

Fig. 1. Hydrothermal occurrences on the Mid-Atlantic Ridge. (1) MAR rift valley and transform faults; (2) hydrothermal ore fields.

smokers that appeared only 3–4 yr ago. These differences in age, intensity, and duration of the activity of sulfide mounds should evidently be reflected in their mineralogical features.

The Logatchev-1 field is characterized by copper specialization of ores and horizontal zonality of mineralization. In the Logatchev-2 and Rainbow fields, zinc ores are more developed, whereas zonality is only detected in the chimneys. The zonality of chimneys has been scrutinized in the Rainbow field (Bogdanov *et al.*, 2002; Borodaev *et al.*, 2004).

Since the hydrothermal fields were discovered in different years, their mineralogy and geochemistry have been investigated in various details. However, the accumulated data make it possible to carry out their comparative analysis. Significant works in this aspect have already been performed in (Bogdanov *et al.*, 2000, 2002; Bortnikov *et al.*, 2001; Fouquet *et al.*, 1998; Lein *et al.*, 2001, 2003; Vikent'ev, 2001; Vikent'ev *et al.*, 2000; and others). In the present communication, we report results of the comparative analysis of specific features of mineral assemblages and their alterations, as well as chemistry and textural–structural relationships of ore minerals, in order to elucidate the influence of the maturity of mounds on the mineralogy and geochemistry of sulfide ores.

Ore samples were taken during several cruises of the R/V *Professor Logatchev*, including Cruise 17 in 1998 (Logatchev-2), and cruise of the R/V *Atlantis* in 2001 (Logatchev and Rainbow fields). We also investigated the material recovered by the manned submersible *Mir-1* during Cruise 47 of the R/V *Akademik Mstislav Keldysh* in 2002 (samples taken by V.I. Starostin) from the Rainbow smoke zone of the youngest active smokers.

Polished sections were prepared from the samples without heating using the method of preliminary treatment with epoxy. The samples were scrutinized on the basis of modern methods of research. Minerals and their textural–structural relationships were investigated in the reflected light under an ore microscope and scanning electron microscopes JEM-100C (Institute of Geology of Ore Deposits, Petrography, Mineralogy, and Geochemistry) and Camscan (Geological Faculty, Moscow State University). The chemical composition was determined using microprobes CAMEBAX-SX-50 (Geological Faculty, Moscow State University) and CAMEBAX MICROBEAN (Moscow State Social University) and electron microscope JEM-110C equipped with energy-dispersive spectrometer Link ISIS (Institute of Geology of Ore Deposits, Petrography, Mineralogy, and Geochemistry). Measurements on CAMEBAX-SX-50 (acceleration 20 kV, beam current 30 nA) were carried out using the following standards (elements, lines): pure metals (CoKα, AuLα, AgLα), CuS (CuKα), FeS (FeKα, SKα), and ZnS (ZnKα). Measurements on CAMEBAX MICROBEAN were performed using the following standards: FeS_2 for Fe (FeKα) and S (SKα) and pure metals for other metals. The probe diameter was 1 μm. The exposure time

Table 1. General characteristics of sulfide mounds related to ultramafic rocks of the MAR (based on our materials and data reported in works of Krasnov *et al.,* 1995; Fouquet *et al.,* 1998; Cherkashev *et al.,* 2000; Bogdanov and Sagalevich, 2002; and Lazareva *et al.,* 2002)

Fields	Date of discovery	Coordinates, N	Depth, m	Age, ka	Dimension and scale of mineralization	Geological setting	Hydrothermal activity	Specialization	Zonality
Logatchev-1	1993–94	14°45′	2860–3040	50–66.5, Cu zone; 3.1–32.2, Fe(Zn) zone	0.3 km^2, 15 ore mounds (dimension of the largest mound 200 m × 100 m), 1750 ka	Tectonic terrace of the eastern slope of rift valley	The major part is inactive; active sectors are located along the NW linear structures within two ore mounds	Cu	Cu zone in the SE area of the mound; Fe(Zn) zone in the NW area
Logatchev-2	1998	14°43,22′	2670–2740	3.9	0.15 km^2, 6 ore mounds (dimension of the largest mound 150 m × 80 m), 250 ka	Small sublatitudinal protrusion ridge on the eastern slope of rift valley	Absent	Cu–Zn(Co,Ni)	Zonality in chimneys
Rainbow	1997	36°14′	2270–2320	22–23 (western sector); 2.2–3.9 (central sector)	0.015 km^2, tens of ore mounds, 500–1000 ka	Large submeridional tectonic rise (protrusion ridge) intersecting rift valley floor in the nontransform dislocation zone between segments of the second order	More than 10 large active mounds and a small number of inactive mounds	Cu–Zn(Co,Ni)	Zonality in chimneys

was increased to 10 s for the determination of trace elements. The identification and crystallochemical features of minerals were refined on the basis of debyegrams (RKD-57.3 and Gandolfi cameras) and diffractograms (Rigaku D/Max-2000/PC automatic diffractometer). The material for these investigations was extracted under a microscope from mineral grains subjected to preliminary microprobe analysis.

MINERAL COMPOSITION

Table 2 shows that major ore minerals in the studied hydrothermal fields belong to the Fe(Zn)–Cu–S system, but their quantitative proportions are variable in different sites. Ores of the Logatchev-1 field are characterized by the predominance of copper minerals (chalcopyrite, isocubanite, bornite, and all minerals of the Cu–S system ranging from covellite to chalcocite). Iron disulfides are also abundant, whereas pyrrhotite is virtually absent. In contrast, ore occurrences of Rainbow and Logatchev-2 are dominated by sphalerite, the presence of pyrrhotite, and the subordinate role of iron disulfides and copper sulfides.

All hydrothermal fields of the studied region are characterized by high concentrations of Co and Ni, presumably, inherited from ultramafic rocks. A small quantity of cobalt and nickel minerals has also been detected in seamounts in Logatchev-1 (Mozgova *et al.*, 1996, 1999) and Rainbow (Lein *et al.*, 2001; Vikent'ev, 2001). These minerals are most widespread in ores of the Rainbow field, resulting in a specific character of their bulk chemical composition. According to Lein *et al.* (2003), the Co concentration in Rainbow ores is 8–10 times higher than that in sulfides of Logatchev-1 and Logatchev-2.

The presence of accessory native metals is a specific feature of the studied objects. Tiny grains of native metals without traces of supergene alteration are sporadically encountered among primary sulfides and nonmetallic minerals in all ores. In addition, the Logatchev-1 field contains an assemblage of native copper, Au-bearing Zn-copper (natural brass), and atacamite related to halmyrolysis (Mozgova *et al.*, 1999). Analogous supergene assemblages were previously reported from mounds of the TAG field (Hannington *et al.*, 1988).

The available data (Bogdanov *et al.*, 2002; Borodaev *et al.*, 2000; Mozgova *et al.*, 1999; and others) suggest that concentrations of trace elements (including noble metals) in ubiquitous ore minerals (sphalerite, iron disulfides, and chalcopyrite) are maximal in young active chimneys of the Rainbow field and are minimal in ores of the much older Logatchev-1 field.

Comparative Characteristics of Major Ore Minerals in Logatchev-1, Logatchev-2, and Rainbow Hydrothermal Mounds

Fe–S and Zn–S Systems. Minerals of this system are represented by pyrrhotite, pyrite, marcasite, and sphalerite.

Pyrrhotite is virtually absent in ores of the Logatchev-1 field. Pyrrhotite pseudomorphs are probably represented by Cu- or Co–Cu-bearing platy iron disulfides and intergrowths of extended sphalerite grains. In contrast, ore occurrences of the Rainbow and Logatchev-2 fields contain abundant pyrrhotite. This mineral is particularly widespread as platy crystals (a few micrometers to 5 mm across) in ores of the Rainbow field, where Bogdanov *et al.* (2002) noted local areas with massive pyrrhotite ores.

In the Rainbow field, the Fe content in pyrrhotite varies from 56.67 to 61.32 wt % (average 59.82 wt %, based on 23 analyses). These values correspond to formula ranging from $Fe_{0.82}S$ to $Fe_{0.91}S$ with variations of coefficient x from 0.18 to 0.09 in the conventional pyrrhotite formula $Fe_{1-x}S$. In the reference data (Chvileva *et al.*, 1988; *Mineraly…*, 1960; Vaughan and Craig, 1978; and others), the deficit of Fe in pyrrhotite is governed by its symmetry. Pyrrhotite with composition ranging from $Fe_{0.86}S$ to $Fe_{0.88}S$ belongs to the monoclinic modification, whereas Fe-rich pyrrhotite with composition ranging from $Fe_{0.90}S$ to $Fe_{0.92}S$ belongs to the hexagonal symmetry. The latter modification is only stable at more than 308°C in experiments with the Fe–S system (Vaughan and Craig, 1978).

Analytical results show that pyrrhotite in the Rainbow field is generally represented by the monoclinic modification, while the hexagonal variety is subordinate. One can observe compositional variations even within separate crystals (e.g., from $Fe_{0.85}S$ at the center to $Fe_{0.91}S$ at the margin. Evidently, the symmetry of such crystals changed in the course of growth. Therefore, they represent a heterogeneous blend of both modifications.

In contrast to pyrrhotite, **pyrite** and **marcasite** are common in all objects studied, but they are particularly widespread in the Logatchev-1 field. Their insignificant compositional variations fit the nonstoichiometry range known for oceanic samples. The maximal Fe variation observed in the Rainbow pyrite is 2.0 at % (from 32.8 to 34.8 at %), which is nearly identical to the interval of 2.1 at % (from 32.3 to 34.4 at %) reported from the oceanic pyrite (Dubut *et al.*, 1982), but it is notably higher than the interval of 1.4 at % (from 33.3 to 34.7 at %) obtained for pyrite in the Logatchev-1 field (Mozgova *et al.*, 1999). The latter interval is similar to the variation of 1.0 at % (from 33.0 to 34.0 at %) recorded in pyrite from ores of the EPR 21°S area (Mozgova *et al.*, 1995a).

Sphalerite is developed in all studied samples. However, this mineral is most abundant in the Logatchev-2 field as grains and aggregates in massive

Table 2. Mineral composition of sulfide mounds related to ultramafic rocks of the MAR (based on our materials and data reported in works of Bogdanov *et al.,* 2002; Lazareva *et al.,* 1998, 2002; Lein *et al.,* 2001, 2003; Torokhov *et al.,* 2002; Vikent'ev *et al.,* 2000)

Minerals	Formula	Logatchev-1	Logatchev-2	Rainbow
Chalcopyrite	$CuFeS_2$	++++	+++	+++
Phase X	$Cu_{0.9}Fe_{1.1}S_2$	+	+	
Pyrrhotite	$Fe_{1-x}S$	+	+++	++++
Troilite	FeS			++
Pyrite	FeS_2	++++	++	++
Marcasite	FeS_2	+++	+++	+++
Sphalerite	(Zn,Fe)S	+++	++++	++++
Isocubanite	$CuFe_2S_3$	+++	+++	++++
Phase Y	$Cu_2Fe_3S_5$	+	+	++
Bornite	Cu_5FeS_4	++++	+++	+++
Phases A and B (orange bornite)	$Cu_{10}Fe_3S_{11}$ and $Cu_{11}Fe_3S_{13}$	++		
Covellite	CuS	+++	++	+
Jarrowite	$Cu_{1.1}S$	++	+	+
Spionkopite	$Cu_{1.4}S$	+	+	++
Geerite	$Cu_{1.5–1.6}S$	++		++
Anilite	$Cu_{1.75}S$	+++		
Digenite	$Cu_{1.75–1.78}S$	++		
Roxbyite	$Cu_{1.72–1.82}S$	+		
Djurleite	$Cu_{1.93–1.96}S$	+++		+
Chalcocite	Cu_2S	+		+++
Chalcocite (tetragonal)	Cu_2S			+
Millerite	NiS			++
Pentlandite	$(Ni,Fe)_9S_8$			++
Co-pentlandite	$(Co,Ni,Fe,Cu)_9S_8$	+++		+
Cobaltite	CoAsS		+	
Arsenides of the lollingite-safflorite series	$FeS_2(Co,Fe)As_2$		+	
Native gold	Au	++	++	+
Electrum	(Au,Ag)		++	
Native silver	Ag	+		
Native copper	Cu	+		
Zn-copper (brass)	$\approx Cu_2Zn$	+		
Native cadmium	Cd			+
Native arsenic	As		+	
Native lead	Pb		+	
Native platinum	Pt(Fe,Cu)			+
Acanthite	Ag_2S			+
Galena	PbS		+	
Sulfoarsenides of Pb,Cu, and Fe	?		+	
Luzonite	Cu_3AsS_4		+	
Tetrahedrite	$Cu_{10}(Fe,Zn)_2Sb_4S_{13}$		+	
Tennantite-tetrahedrite	$Cu_{10}(Fe,Zn)_2(As,Sb)_4S_{13}$		+	
Tennantite	$Cu_{10}(Fe,Zn)_2As_4S_{13}$	+	+	
Coloradoite	HgTe		+	+
Molybdenite	MoS_2			+
Cu–Fe–Co-disulfide	$Cu(Fe,Co)_9S_{20}$	+		
Cu–Fe-disulfide	$(Fe_{0.95}Cu_{0.05})S_2$	+		
Magnetite	Fe_3O_4			+
Hematite	Fe_2O_3	++		
Iron hydroxides	?	++	++	+++
Uraninite	UO_2		+	
Cassiterite	SnO_2			+

Note: (++++) Major; (+++) subordinate; (++) rare; (+) very rare.

ores, as well as porous and druse-shaped aggregates on conduit walls. In contrast to the chalcopyrite-free counterpart in ancient smokers of the Logatchev-1 field, sphalerite in young chimneys of Logatchev-2 and Rainbow commonly includes chalcopyrite emulsion and often makes up intergrowths with chalcopyrite.

In all three hydrothermal fields, the sphalerite composition shows a wide compositional range owing to variations in the Fe content (from 0.*n* to 25 wt %, based on 37 analyses). In the Rainbow sphalerite, the Fe content is maximal and considerably variable even within separate crystals. The Fe content decreases from the grain center to margin (e.g., from 22.0 to 6.5 wt %). In the Logatchev-1 field, the Fe content in sphalerite displays an inverse correlation with the chemical specialization of zones: the maximal Fe content (14–16 wt %) is found in the copper zone, while the minimal content (3–6 wt %) is typical of the Fe(Zn)-rich zone (Mozgova *et al.*, 1999).

Cu–Fe–S System. The Cu–Fe–S system is most interesting, because its central part includes the major ore-forming sulfides that are highly sensitive to variations in physicochemical conditions. These minerals are best studied and very informative. It is also worth noting that the Cu–Fe–S system with a very important geological significance has been experimentally investigated in many laboratories of the world, and the accumulated experimental material is useful for the investigation of natural assemblages.

Among the major minerals in the central part of the Cu–Fe–S system, we studied chalcopyrite, isocubanite, bornite, and orange bornite. Special attention was devoted to two new phases X and Y (Mozgova *et al.*, 2002a) discovered during the examination of laths in exsolution structures of isocubanite or intermediate solid solution (phase iss). The latter term was first introduced by Merwin and Lombard (1937) based on the study of the Cu–Fe–S system. The composition of phases X and Y is intermediate between chalcopyrite and isocubanite. Therefore, we consider phases X and Y as modifications of these minerals.

Chalcopyrite is observed as homogenous grains and crystals among other sulfides and as aggregates of small crystals on walls of active chimneys. In all three hydrothermal fields, the chalcopyrite composition is nearly similar and insignificantly differs from the theoretical formula. Variation in the content of major elements is as follows (wt %): Cu 31.80–34.98, Fe 29.99–31.80, and S 34.09–36.00. Based on 50 analyses, the average content is as follows (wt %): Cu 34.00, Fe 30.37, and S 34.91. Deviation from the theoretical chalcopyrite composition (Cu 25, Fe 25, and S 50 at %) does not exceed 1 at %. This deviation fits the nonstoichiometry range of chalcopyrite from continental deposits (up to 2.4 at %) based on the processing of reference data on chalcopyrite composition in continental deposits (Lafitte and Maury, 1982).

The **readily oxidizable chalcopyrite** was only found in active small zonal chimneys crowning young larger chimneys of the Rainbow field. Chalcopyrite makes up a zone up to 5–8 mm wide at the contact with the older phase Y on the chimney wall. In near-contact areas, the chalcopyrite is developed as lamellae in phase Y matrix of latticed structures (Fig. 2) that are obviously products of the decomposition of metastable solid solution related to the diffusion of metals at the contact. In freshly prepared thin sections, the oxidizable variety is similar (in color and shape of reflection dispersion curve) to ordinary chalcopyrite, although the reflectivity (*R*) is 10–15% lower (Fig. 3a). The mineral is rapidly oxidized in atmosphere and becomes pinky brown. The *R* value is appreciably lower (by 20–25% in the longwave region of the spectrum), and the dispersion curve has a reversed slope similar to that of digenite and chalcocite (Fig. 3b). Variation of its microhardness (114–235 kgs/mm^2) is considerably higher than that of ordinary chalcopyrite (181–203 kgs/mm^2).

Table 3 shows that the oxidizable chalcopyrite has the following composition (wt %): Cu 31.23–34.75, Fe 27.87–32.26, and S 34.98–36.03. This composition can be recalculated into the formula $CuFeS_2$ with formula coefficients of Cu and (Fe + Co + Ni) equal to 0.91–1.01 and 0.99–1.08, respectively. Thus, the general empirical formula of this mineral can be written as $Cu_{1-x}(Fe,Co,Ni)_{1+x}S_2$, where x varies from 0 to 0.09. At the maximal value of x (0.09), the end member of the studied system has the following composition (at %): Cu 22.75, Fe 27.25, and S 50.00. Deviation from the ideal composition (Cu 25, Fe 25, and S 50 at %) is 2.25 at %. The Me/S ratio is close to unity. In the Cu–Fe–S ternary diagram (Fig. 4), data points should be located between ideal compositions of chalcopyrite and phase X on the tie line with Me/S = 1 (not shown in the diagram). Thus, the composition of the studied mineral fits the nonstoichiometry range (2.4 at %) of chalcopyrite from continental deposits (Lafitte and Maury, 1982) and virtually matches the narrow field of chalcopyrite solid solution (css) ranging from $CuFeS_2$ to $Cu_{0.9}Fe_{1.1}S_2$ in experimental hydrothermal systems at 350 and 300°C (Sugaki *et al.*, 1975). Hence, despite the isotropism, high oxidizability, and low values of reflectivity and microhardness, the studied chalcopyrite compositionally does not differ from ordinary natural and synthetic varieties.

The XRD study made it possible to outline some differences. The XRD pattern of the studied mineral fits standard data on the tetragonal chalcopyrite. However, some reflections typical of the tetragonal symmetry are significantly broader. At the same time, the high-angle strong reflections correspond to reflections of cubic chalcopyrite and can be indexed in the cubic lattice. Hence, the cation distribution in sulfur tetrahedra in the studied mineral differs little from the cubic pattern. In the ordinary tetragonal chalcopyrite, Cu and Fe atoms occupy strictly regular positions, whereas they are completely disordered in the cubic chalcopyrite. The vague-

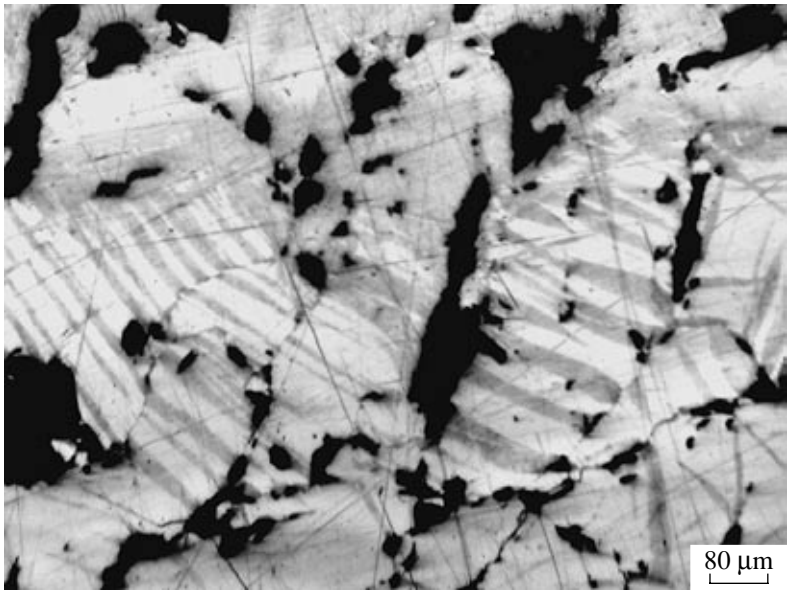

Fig. 2. Exsolution lattice structure at the boundary of two zones composed of phase Y and readily oxidizable chalcopyrite in the copper chimney (Rainbow). Polished section, reflected light. Chalcopyrite and phase Y make up lamellae (gray) and matrix (white).

ness of XRD reflections, which define the tetragonal symmetry of mineral, suggests an incomplete ordering of cations in various sites.

The data obtained make it possible to suppose the following oxidation mechanism for the studied mineral. In the chalcopyrite formula $Cu^{+}Fe^{3+}S_2$, Fe is already in the highest oxidation state, whereas Cu is in the monovalent state (Vaughan and Craig, 1978). Hence, only Cu can be subjected to oxidation ($Cu^{+} \longrightarrow Cu^{2+}$) in the chalcopyrite. In order to preserve the balance of charges, the excess of Cu^{+} atoms released during oxidation diffuses to the thin section surface and produces a film of Cu-rich sulfides of the chalcocite–digenite series characterized by the prevalence of monovalent Cu. This scenario is supported by the similarity of reflection dispersion curves of chalcopyrite (with oxidized coating) and copper sulfides of the chalcocite–digenite series, as well as by the appearance of some weak reflections in the powder XRD image of the studied chalcopyrite that are similar to reflections in the standard powder XRD images of these sulfides. Thus, oxidation of Cu is accompanied by its diffusion, which is typical of this element in crystal structures of sulfides.

Phase X (anomalous chalcopyrite) is only represented by lamellae in the isocubanite matrix. In the Rainbow field, this phase could not be analyzed because of very small size of lamellae. The chemical composition of lamellae in ores of the Logatchev-1 field is as follows (wt %): Cu 31.55, Fe 32.18, S 34.48, and total 98.16. In the Logatchev-2 field, the contents are as follows: Cu 31.48, Fe 32.33, S 35.03, and total 98.84 (Table 4). Thus, the average composition differs from the theoretical composition of chalcopyrite by approximately 3 wt % (in terms of metal contents) and is close to formula $Cu_{0.9}Fe_{1.1}S_2$. Deviations of Cu and Fe concentrations from the ideal version are equal to ±2.5 at %, which exceeds the nonstoichiometry region of ordinary chalcopyrite (±1 at %). Therefore, the studied phase X can be regarded as a nonstoichiometric variety of chalcopyrite.

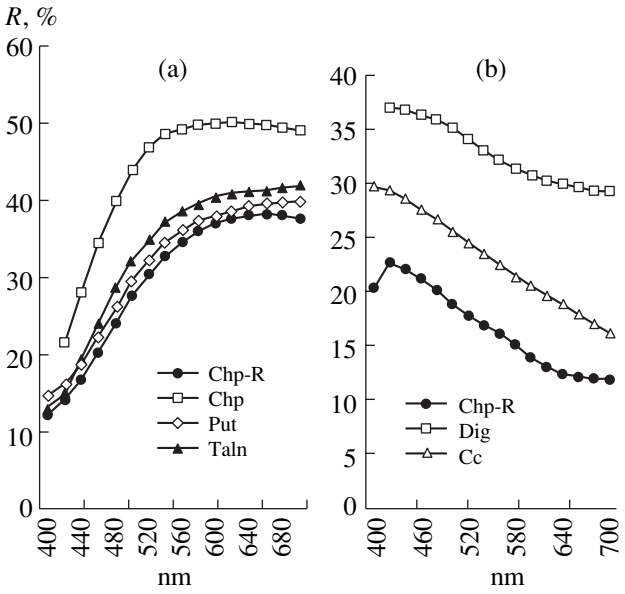

Fig. 3. Reflection dispersion curves of readily oxidizable chalcopyrite as compared to literature data (Chvileva *et al.*, 1988). (a) Freshly prepared readily oxidizable chalcopyrite from the Rainbow field (Chp-R), putoranite (Put), talnakhite (Taln), and standard chalcopyrite (Chp); (b) readily oxidizable chalcopyrite from the Rainbow field with oxidation coating (Chp-R), digenite (Dig), and chalcocite (Cc).

Table 3. Chemical composition of readily oxidizable chalcopyrite from the Rainbow field, wt % (based on microprobe data)

Sample no.	Analysis no.	Cu	Au	Ag	Fe	Co	Ni	Zn	S	Total
Homogenous chalcopyrite										
4412-10	8	31.23	0.37	–	27.87	3.56	1.49	–	35.06	99.58
	6	32.39	0.24	0.10	32.36	0.34	0.20	0.02	35.53	101.18
4412-9	6a	33.35	–	0.03	31.45	n.d.	n.d.	–	35.77	100.60
	5	33.56	–	–	32.16	n.d.	n.d.	–	35.68	101.40
	32*	34.09	–	–	31.22	n.d.	n.d.	–	36.03	101.34
4412-10	9	34.17	0.09	–	30.07	0.11	0.25	0.12	35.38	100.19
4412-6	15*	34.75	–	–	30.25	n.d.	n.d.	–	34.56	99.56
Average		33.36	0.10	0.02	30.77	0.57	0.28	0.02	35.43	100.55
Lamellae										
4412-9	7(L)	32.63	0.40	–	31.85	n.d.	n.d.	0.02	35.55	100.45
4412-6	43(L)	33.01	–	0.03	31.75	n.d.	n.d.	0.15	35.64	100.58
	40(L)	33.21	–	–	31.42	n.d.	n.d.	0.02	34.98	99.63
Average		32.63	0.13	0.01	31.42	0.06			35.39	100.22
Isochalcopyrite (Atlantis II, Red Sea) (Missack *et al.,* 1989)										
Homogenous		34.04	–	–	32.20	–	–	0.15	33.87	100.26
Lamellae (grain center)[2]* (L-1)		31.69	–	–	34.51	–	–	0.20	33.85	100.25
Lamellae (grain edge)[3]* (L-2)		33.08	–	–	32.81	–	–	0.26	33.88	100.03
Composition of minerals of the chalcopyrite group (Anthony *et al.,* 1990)										
Chalcopyrite $CuFeS_2$		34.56			30.52				34.92	100.00
Putoranite[4]* $Cu_{18}(Fe,Ni)_{18}S_{32}$		35.68			31.22		0.51		32.49	99.9
Putoranite[5]* $Cu_{16}(Fe,Ni)_{19}S_{32}$		32.99			32.11		1.63		33.14	99.87
Talnakhite $Cu_9(Fe,Ni)_8S_{16}$		37.15			29.10		0.75		33.31	100.31
Mooihoekite $Cu_9Fe_9S_{16}$		36.02			31.66				32.32	100
Haycockite $Cu_4Fe_9S_8$		32.18			35.35				32.47	100

Formula coefficients (based on 4 atoms in the formula)

Analysis no.	Cu	Fe	Co	Ni	Zn	ΣFe, Co, Ni	S	ΣMe	Me/S	Cu/Fe
Homogenous chalcopyrite										
8	0.90	0.92	0.11	0.05		1.08	2.01	1.99	0.99	0.83
6	0.92	1.05	0.01	0.01		1.07	2.01	1.99	0.99	0.86
6a	0.95	1.02				0.95	2.02	1.98	0.98	0.93
5	0.95	1.04				1.04	2.01	1.99	0.99	0.91
32*	0.97	1.01				1.01	2.03	1.97	0.97	0.96
9	0.98	0.98		0.01		0.99	2.02	1.98	0.98	0.99
15*	1.01	1.00				1.00	1.99	2.01	1.01	1.01
Average	0.96	1.00	0.02	0.01		1.03	2.01	1.99	0.98	0.93
Lamellae										
7(L)	0.94	1.04				1.04	2.02	1.98	0.98	0.90
43(L)	0.94	1.03				1.03	2.02	1.98	0.98	0.91
40(L)	0.96	1.03				1.03	2.00	1.99	1.00	0.93
Average	0.95	1.04				1.04	2.02	1.99	0.99	0.91
Isochalcopyrite (Atlantis II, Red Sea) (Missack *et al.,* 1989)										
Homogenous	0.99	1.06					1.95	2.05	1.05	0.93
L-1	0.92	1.14			0.01		1.94	2.07	1.07	0.80
L-2	0.96	1.08			0.01		1.95	2.05	1.05	0.88

Note: Analyzed by I.A. Bryzgalov (CAMEBAX, Moscow State University); * analyzed by N.V. Trubkin (Link, IGEM); [2]* average of 5 analyses; [3]* average of 3 analyses; [4]* average of 7 analyses; [5]* average of 12 analyses; (–) absent; (n.d.) not determined.

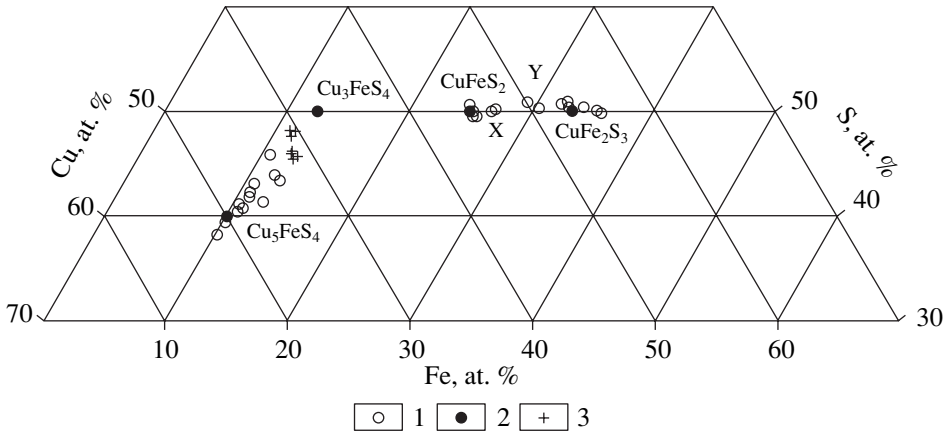

Fig. 4. The Cu–Fe–S diagram for copper and iron sulfides. (1) Compositions of analyzed sulfides; (2) theoretical compositions; (3) compositions of phases A and B (orange bornite).

In reflected light under a microscope, phase X demonstrates weak anisotropy (from bluish gray to pinky brown) that is typical of the ordinary tetragonal chalcopyrite. This effect is well observed in lamellae among the isotropic isocubanite matrix.

Comparison with experimental data on the hydrothermal Cu–Fe–S system (Sugaki *et al.,* 1975) shows that phase X corresponds to the css end member. At 350°C, it makes up a narrow band along the Me/S ≈ 1 line with composition varying from the nearly stoichiometric $CuFeS_2$ to $Cu_{0.9}Fe_{1.1}S_2$. Similar sizes of the css domain, which also extends toward higher Fe values, has been reported for the Cu–Fe–Zn–S system (Ueno *et al.*, 1980).

Normal and isotropic varieties of chalcopyrite have been reported from sulfide sediments of the Atlantis II Deep in the Red Sea (Missack *et al.*, 1989). The isotropic variety was named isochalcopyrite and tentatively considered an equivalent of the high-temperature cubic chalcopyrite. The mineral was observed as lamellae in exsolution structures of phase iss and as separate homogenous grains. Analytical results indicate that

Table 4. Chemical composition of lamellae of phase X (anomalous chalcopyrite) in iss exsolution structures of the Logatchev-1 and Logatchev-2 fields (based on microprobe data)

Sample no.	Analysis no.	Content, wt %				Formula (based on 4 atoms)
		Cu	Fe	S	Total	
Logatchev-1						
9	1	31.12	32.44	34.38	97.94	$Cu_{0.91}Fe_{1.08}S_{2.00}$
	2	31.71	32.02	34.16	98.06*	$Cu_{0.93}Fe_{1.07}S_{1.9}$
	3	31.81	32.09	34.65	98.55	$Cu_{0.93}Fe_{1.07}S_{2.01}$
Average of 3 analyses		31.55	32.18	34.40	98.16	$Cu_{0.93}Fe_{1.07}S_{2.00}$
Logatchev-2						
384-4	4	31.01	33.64	34.54	99.19	$Cu_{0.90}Fe_{1.11}S_{1.99}$
	5	31.19	33.20	34.60	98.99	$Cu_{0.91}Fe_{1.10}S_{1.99}$
	6	31.47	32.70	34.77	98.94	$Cu_{0.91}Fe_{1.08}S_{2.00}$
	7	31.49	31.92	35.00	98.41	$Cu_{0.92}Fe_{1.06}S_{2.02}$
	8	31.56	32.23	35.08	98.87	$Cu_{0.92}Fe_{1.06}S_{2.02}$
	9	31.76	32.36	35.11	99.23	$Cu_{0.92}Fe_{1.07}S_{2.01}$
	10	31.93	32.21	35.24	99.38	$Cu_{0.92}Fe_{1.06}S_{2.00}$
	12	31.42	33.25	35.88	101.48[2]*	$Cu_{0.89}(Fe_{1.07}Zn_{0.03})_{1.10}S_{2.01}$
Average of 8 analyses		31.48	32.33	35.03	98.84	$Cu_{0.91}Fe_{1.07}S_{2.02}$
Theoretical		31.30	33.61	35.09	100.00	$Cu_{0.9}Fe_{1.1}S_{2.0}$

Note: * Zn 0.05, Au 0.12; [2]* Zn 0.93.

Table 5. Chemical composition of isocubanite from the Rainbow and Logatchev-1 fields (based on microprobe data)

Average of	Content, wt %				Total	Formula (based on 6 atoms)	Cu/Fe	Note
	Cu	Fe	Zn	S				
Rainbow (homogenous)								
6 analyses	20.78	43.05	0.06	35.56	100.02	$Cu_{0.88}Fe_{2.09}Co_{0.03}S_{3.00}$	0.42	Co 0.57 wt %
Logatchev-1 (matrix)								
3 analyses	21.24	41.22	0.09	35.01	97.56	$Cu_{0.92}Fe_{2.05}S_{3.03}$	0.45	Station 9
5 analyses	19.91	43.33	0.37	34.86	98.47	$Cu_{0.89}(Fe_{2.14}Zn_{0.02})_{2.16}S_{2.98}$	0.40	Station 2

isochalcopyrite differs from phase X in both optical properties and chemical composition. The isochalcopyrite is enriched in metals and depleted in sulfur, relative to phase X (Me/S = 1.06 and 0.98–1.0, respectively).

Isocubanite, a high-temperature cubic modification of the orthorhombic cubanite $CuFe_2S_3$, was identified as a mineral species during the study of sulfides from black smokers in the EPR 21° N area and from metalliferous sediments in the Red Sea (Caye *et al.*, 1988). Isocubanite had previously been known under various names in continental and oceanic ores. This mineral is considered a natural analogue of phase iss. In contrast to the very narrow nonstoichiometry region of chalcopyrite, the iss composition field remains wide at 350–350°C (Sugaki *et al.*, 1975 and others). Overview of data on chemistry of the oceanic isocubanite also revealed a wide compositional field. Variation of the Cu/Fe ratio in this mineral at a constant Me/S value can be defined by formula $(Cu_{1-y}Fe_{2+y})_3S_3$, where $0.56 \le y \le 0.20$ (Mozgova *et al.*, 1995b).

In the studied samples from Logatchev-1 and Logatchev-2 fields, isocubanite was only found as matrix in latticed iss exsolution structures. The matrix includes lamellae commonly represented by anomalous Fe-rich chalcopyrite (in some cases, by isocubanite enriched in Cu relative to the ideal formula $CuFe_2S_3$). These modifications were called phases X and Y, respectively (Mozgova *et al.*, 2002a).

In the Rainbow field, isocubanite is represented by two varieties. The first variety is present among very fine latticed exsolution structures (commonly, in association with sphalerite). The homogenous variety associated with iron sulfides, occasionally, makes up aggregates of euhedral crystals on conduit walls (Fig. 5a). Results of the comprehensive analysis of this phase have been reported in (Mozgova *et al.*, 2002b). In the present communication, we shall only give a brief comparative description of chemical features of this mineral.

The chemical composition of homogenous isocubanite from the Rainbow field corresponds to formula $Cu_{0.88}Fe_{2.09}Co_{0.03}S_{3.00}$ (average of six analyses). This composition is similar to that of isocubanite matrix in samples from the Logatchev-1 field (Table 5). In both cases, isocubanite is depleted in Cu (by 2–3 wt %), relative to the nearly ideal composition observed in the isocubanite matrix from the Logatchev-2 field. Thus, isocubanites in the studied objects vary from the nearly ideal composition to the notably Fe-rich variety. The compositional variation can be defined as $Cu_{1-x}Fe_{2+x}S_3$, where $0.04 \le x \le 0.14$. The Cu/Fe variation range (0.40–0.53) is comparable to that in isocubanite (0.44–0.59) in black smokers (Mozgova *et al.*, 1995b). In the Cu–Fe–S diagram (Fig. 4), our data points lie on the tie line with Me/S ≈ 1 near the ideal isocubanite composition with Cu/Fe = 0.5.

Thus, the results obtained suggest that the primary homogenous isocubanite had a variable composition. Lamellae related to its exsolution are enriched in Cu. Hence, relative to the Rainbow counterpart, the metastable phase iss was enriched in Cu during its precipitation from inactive smokers of Logatchev-1 and Logatchev-2.

Interestingly, Wintenberger *et al.* (1994) have reported isocubanite matrix from the Snake Pit area (MAR 23° N) as a new phase $CuFe_3S_4$. This is the highest Fe content recorded in the isocubanite matrix. Based on the above formula, the Cu/Fe ratio in the mineral is 0.33, which approaches the lowermost Cu/Fe value known for isocubanites in sulfide muds (0.36–0.95) (Mozgova *et al.*, 1995b). Thus, isocubanites from submarine sulfide ores are characterized by a very wide variation range.

Phase Y, compositionally similar to isocubanite, was discovered in ores of Logatchev-1 and Logatchev-2 as lamellae in iss exsolution structures (Mozgova *et al.*, 2002b). In the Rainbow field, this phase is observed not only as lamellae among iss exsolution products (in association with sphalerite), but also as homogenous segregations in active zonal copper chimneys in association with the readily oxidizable chalcopyrite described above (Borodaev *et al.*, 2004b). In these chimneys, phase Y makes up the first zone around the chimney. This zone (200 μm to 2 mm wide) displays a radial-fibrous texture of elongate grains (50–150 μm) of phase Y.

With respect to reflectivity and color, phase Y is indiscernible from the freshly polished sample of readily oxidizable chalcopyrite in the contact zone. Boundary between the two phases can only be outlined by the microprobe analysis or after the tarnishing of chalcopyrite in atmosphere (Fig. 3). In the freshly pre-

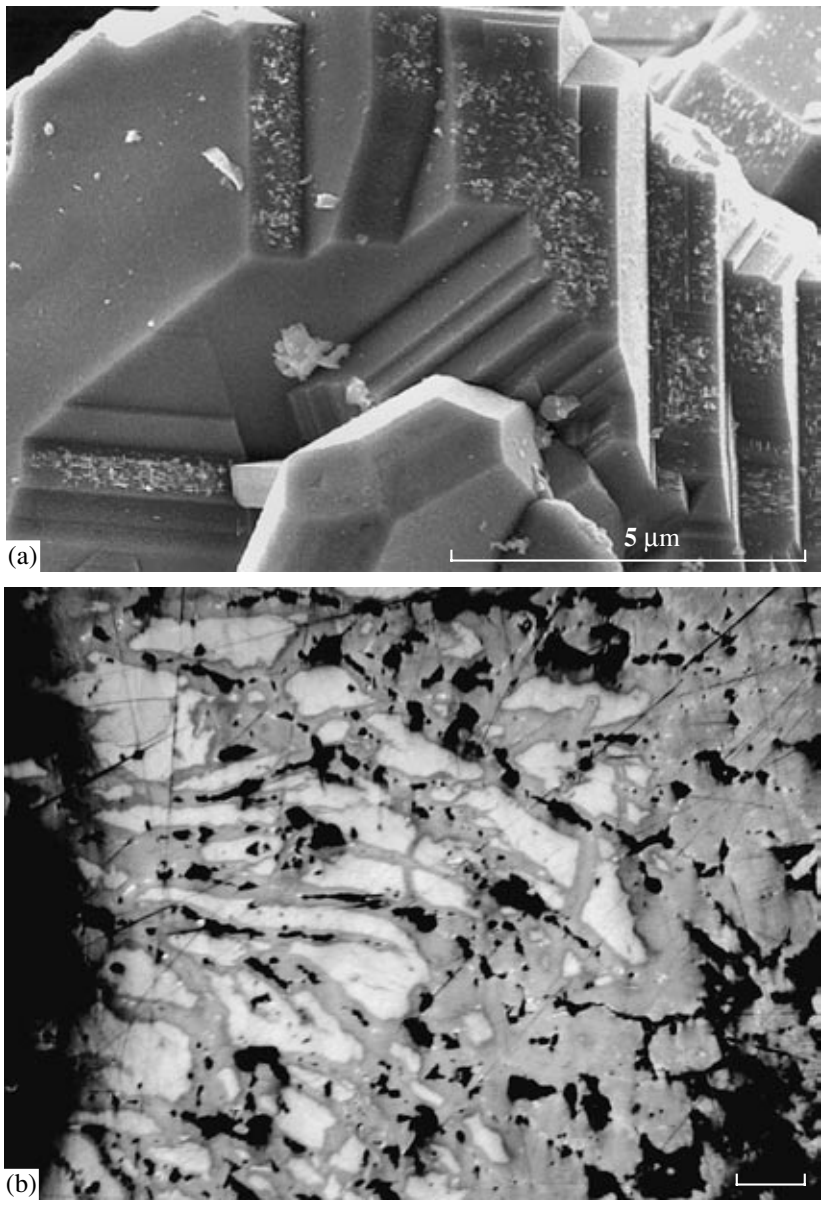

Fig. 5. Isocubanite and bornite segregations in the studied ores (Rainbow field). (a) SEM image of homogenous isocubanite on chimney walls. One can see crystal growth terraces and tiny isocubanite crystallites of later generation at their ends. An idiomorphic iron disulfide crystal is observed in the lower part of the photomicrograph. (b) Replacement of chalcopyrite (white) by bornite (gray). Black spots are pores and defects related to polishing. Polished section, reflected light.

pared polished sections, phase Y has a lower reflectivity relative to chalcopyrite, although the difference is not noted during the macroscopic examination. Anisotropy is also absent.

Phase Y from the Rainbow field was investigated using two different microprobes (18 analyses) and the results turned out to be rather similar (Table 6). They are characterized by the universal presence of Co and Ni (0.*n* wt %) and the sporadic presence of Au (up to 0.28 wt %) and Ag (traces). The averaged calculated formula $Cu_{2.00}(Fe_{2.94}Co_{0.04}Ni_{0.03})_{3.01}S_{4.99}$ is nearly stoichiometric and similar to data on laths from iss exsolution structures in the Logatchev-2 field. Relative to isocubanite, the ideal composition of phase Y ($Cu_2Fe_3S_5$) is enriched in Cu (consequently, depleted in Fe) by approximately 4.5 wt % at nearly similar sulfur contents. It should be emphasized that phase $Cu_2Fe_3S_5$ had previously been identified in nodules of enstatitic chondrites in association with the Ga-bearing sphalerite (Rambaldi *et al.*, 1986).

In the Cu–Fe–S diagram (Fig. 4), data points of phase Y are clustered near the point of Cu/Fe = 0.66 (interval 0.63–0.68). In terms of the ratio of cations (Cu/Fe ≈ 0.7), phase Y approaches haycockite $Cu_4Fe_5S_8$

Table 6. Chemical composition of homogenous phase Y from copper chimneys of the Rainbow field and of lamellae in exsolution structures of the Logatchev-2 field (based on microprobe data) as compared to literature data (wt %)

Analysis no.	Cu	Au	Ag	Fe	Co	Ni	Zn	S	Total	Formula (based on 10 atoms)	Me/S	Sample no.
15	29.44	0.06	0.06	34.99	0.54	0.16	0.02	35.25	100.52	$Cu_{2.10}(Fe_{2.85}Co_{0.04}Ni_{0.01})_{2.90}S_{4.99}$	1.00	4412-10
12	29.14	0.26	0.08	34.68	0.60	0.13	0.11	35.58	100.58	$(Cu_{2.08}Au_{0.01})_{2.09}(Fe_{2.82}Co_{0.04}Ni_{0.01}Zn_{0.01})_{2.88}S_{5.03}$	0.99	"
14	29.00	–	0.01	35.14	0.67	0.04	–	35.19	100.05	$Cu_{2.08}(Fe_{2.87}Co_{0.05})_{2.92}S_{5.00}$	1.00	"
17	28.73	–	–	34.92	0.57	0.12	0.06	35.31	99.71	$Cu_{2.06}(Fe_{2.85}Co_{0.05}Ni_{0.01})_{2.91}S_{5.03}$	0.99	"
5	28.62	–	0.02	35.35	0.42	0.19	0.06	35.19	99.85	$Cu_{2.05}(Fe_{2.89}Co_{0.03}Ni_{0.02})_{2.94}S_{5.01}$	1.00	"
11	28.56	0.28	–	35.30	0.69	0.01	–	35.34	100.18	$(Cu_{2.04}Au_{0.01})_{2.05}(Fe_{2.88}Co_{0.05})_{2.93}S_{5.02}$	0.99	"
18	28.60	0.08	0.01	35.79	0.78	0.08	0.15	35.28	100.77	$Cu_{2.04}(Fe_{2.90}Co_{0.06}Ni_{0.01}Zn_{0.01})_{2.98}S_{4.98}$	1.01	"
16	28.56	–	0.07	35.54	0.52	0.06	0.13	35.44	100.32	$Cu_{2.04}(Fe_{2.89}Co_{0.04}Zn_{0.01})_{2.94}S_{5.02}$	0.99	"
4	28.21	–	0.02	35.92	0.59	0.11	0.12	36.01	100.98	$Cu_{2.00}(Fe_{2.89}Co_{0.04}Ni_{0.01}Zn_{0.01})_{2.95}S_{5.05}$	0.98	"
43	27.10	–	–	36.95	0.44	0.62	–	34.88	99.99	$Cu_{1.94}(Fe_{3.02}Co_{0.03}Ni_{0.05})_{3.10}S_{4.96}$	1.02	4393-2
25	27.67	0.24	–	36.66	0.39	0.47	0.02	34.54	99.99	$(Cu_{1.99}Au_{0.01})_{2.00}(Fe_{3.00}Co_{0.03}Ni_{0.04})_{3.07}S_{4.93}$	1.03	"
23	27.38	–	–	36.38	0.42	0.41	0.01	34.09	98.69	$Cu_{2.00}(Fe_{3.02}Co_{0.03}Ni_{0.03})_{3.08}S_{4.92}$	1.03	"
42*	27.38	–	–	36.88	0.05	0.26	–	34.78	99.35	$Cu_{1.98}(Fe_{3.03}Ni_{0.02})_{3.05}S_{4.97}$	1.01	"
28	27.36	–	–	35.56	0.76	0.51	–	35.26	99.45	$Cu_{1.97}(Fe_{2.91}Co_{0.06}Ni_{0.04})_{3.01}S_{5.02}$	0.99	"
44	26.83	–	–	37.16	0.46	0.73	0.12	34.97	100.00	$Cu_{1.93}(Fe_{3.03}Co_{0.04}Ni_{0.06}Zn_{0.01})_{3.14}S_{4.93}$	1.03	"
24	26.79	0.14	–	36.51	0.38	0.44	–	34.81	99.07	$Cu_{1.94}(Fe_{3.00}Co_{0.03}Ni_{0.03})_{3.06}S_{4.99}$	1.00	"
45*	26.68	–	–	36.50	0.39	0.78	0.24	34.36	98.95	$Cu_{1.94}(Fe_{3.01}Co_{0.03}\ Ni_{0.06}Zn_{0.02})_{3.12}S_{4.94}$	1.02	"
41	26.38	–	–	37.01	0.62	0.62	0.11	35.27	100.01	$Cu_{1.89}(Fe_{3.01}Co_{0.05}\ Ni_{0.05}Zn_{0.01})_{3.11}S_{5.00}$	1.00	"
Average of 18 analyses	27.91	0.06	0.02	35.96	0.52	0.32	0.06	35.07	99.91	$Cu_{2.00}(Fe_{2.94}Co_{0.04}Ni_{0.03})_{3.01}S_{4.99}$	1.00	"
Lamellae (average of 4 analyses)	27.20	0.10	–	34.96	–	–	0.61	35.46	98.33	$Cu_{1.97}(Fe_{2.89}Zn_{0.04})_{2.93}S_{5.10}$	0.96	Logatchev-2
Cu-sulfide	27.5	–	–	36.4	–	–	–	35.1	99.64[2]*	$Cu_{1.98}(Fe_{2.98}Mn_{0.05})_{3.02}S_{5.00}$	1.00	Nodules in chondrite[3]*
Phase iss	26.3	–	–	38.4	–	–	–	35.1	99.8	$Cu_{1.88}Fe_{3.13}S_{4.99}$ (~$Cu_{1.9}Fe_{3.1}S_{5.0}$)	1.00	Synthesis[4]*
Phase Y	27.93			36.83				35.24	100	$Cu_2Fe_3S_5$	1.00	Theoretical
Isocubanite	23.4			41.2				35.4	100	$CuFe_2S_3$	1.00	Theoretical

Note: * Ce 0.23, La 0.42 (analysis 42); Ce 0.47, La 0.45 (analysis 45); [2]* Mn 0.64 wt %; [3]* (Rambaldi *et al.,* 1986); [4]* (Sugaki *et al.,* 1975).

(Cu/Fe = 0.80), but the haycockite is depleted in sulfur and located below the tie line with Me/S = 1. Data point corresponding to the ideal composition $Cu_2Fe_3S_5$ is shifted from the stoichiometric formula of isocubanite toward chalcopyrite.

Comparison of data obtained with results of the generalization of isocubanite composition in submarine ores (Mozgova *et al.*, 1995b) showed that phase Y falls out from the variation interval of the Cu/Fe ratio typical of isocubanite in black smokers. At the same time, isocubanite from sulfide muds of the Red Sea is characterized by a wide Cu/Fe ratio variation range that includes the data on phase Y. Therefore, one can suppose that phase Y is present in muds of the Red Sea.

In accordance with the Mössbauer data, valent states in cubanite are reflected by formula $Cu^+(Fe^{2+},Fe^{3+})_2S_3$ (Vaughan and Craig, 1978). This statement is obviously valid for isocubanite as well. Taking into consideration the ratio of valence-variable cations in the above formula at Me/S ≈ 1, one can assume that relative to the Cu-depleted isocubanite matrix, phase Y contains a higher amount of oxidized Fe (Fe^{3+}).

Bornite has a long history of study since its discovery in 1845. Nevertheless, some characteristics of this mineral, particularly its chemistry, remain unclear. In the available handbooks (Anthony *et al.*, 1990; *Mineraly…*, 1960; and others), bornite is supposed to have the stoichiometric formula Cu_5FeS_4, but the contents of elements are characterized by variation up to 7–15 wt % (*Mineraly…*, 1960). The variation range is consistent with the large field of the bornite solid solution (bss) in the Cu–Fe–S system known from experimental data (Cabri, 1973; Sugaki *et al.*, 1975; Yund and Kullerud; 1966; and others). In continental deposits, bornite is a common mineral formed in a wide temperature range under both hypogene and supergene conditions (*Mineraly…*, 1960). Bornites can differ in reflected color and chemical composition. For example, cupriferous sandstones of Dzhezkazgan contain not only the normal bornite Cu_5FeS_4 (lilac-colored in reflected light), but also the Cu-rich pink bornite and the orange variety with an excess of S and Fe (Lur'e and Gablina, 1976; Satpaeva and Polkanova, 1978; Satpaeva *et al.*, 1974; and others). The orange variety turned out to be identical to *x*-bornite obtained in experiments with the Cu–Fe–S system at <140°C (Yund and Kullerud, 1966). In the Lubin copper mine (Poland), the *x*-bornite, described as a product of the low-temperature (<40°C) alteration of sulfides, partially decomposes into covellite and chalcopyrite. Its composition varies from $Cu_{4.5}FeS_4$ до $Cu_{3.5}FeS_4$ (Large *et al.*, 1995). Similar anomalous bornite was reported as a compositionally variable supergene metastable phase in (Sillitoe and Clark, 1969).

In oceanic ores, bornite usually leads the group of successively replacing sulfides with the highest Cu content. This pattern is also observed in all the studied objects. Bornite is most abundant in the Logatchev-1 field in three major assemblages. In compact ores, the mineral intensely replaces and crosscuts chalcopyrite in the form of veinlets often containing tiny Co-pentlandite dissemination. Bornite, in turn, is crosscut by thin stringers of copper sulfides. In breccia-type porous sectors, bornite and chalcocite make up thin zonal rims around the relict chalcopyrite and thin zones adjacent to chalcopyrite grains. At the periphery of small chalcopyrite-rich chimneys, bornite occurs in a different assemblage. Together with covellite and other copper sulfides, the bornite is developed after chalcopyrite around hollow cracks oriented from the chimney surface toward the center. In places, the bornite is developed as lamellae in the covellite matrix.

In samples from the Logatchev-2 field, bornite is mainly confined to porous sectors of chalcopyrite and sphalerite–chalcopyrite ores. The mineral is often present on walls of conduits. It is developed along fine cracks and joints in chalcopyrite and iron sulfide grains as diverse replacement (corrosion, reticulate, stringer, comb-shaped, and so on) structures.

In the Rainbow field, bornite is present in zonal walls of young active copper chimneys as an intermittent zone sandwiched between the readily oxidizable chalcopyrite and copper sulfide. Bornite is developed as fine crosscutting stringers oriented toward chalcopyrite grains (Fig. 5b) and as matrix with lamellae of the readily oxidizable chalcopyrite in latticed exsolution structures. On the opposite side, bornite is successively replaced by copper sulfides. The copper sulfide zone is commonly preceded by a thin band of bornite and copper sulfide blend developed along the boundary of zones.

The studied bornite is characterized by a wide composition range. In Table 7, one can see average contents of elements and their variation range in different (pink, normal, and orange) varieties of bornite. It is worth noting that the subdivision of bornites is rather conventional, because they show a gradual transition in composition and reflected color. The compositional field defined by the Cu/Fe ratio of 3.3–6.2 in our work is close to phase bss synthesized at 350°C (Sugaki *et al.*, 1975).

Table 7 shows that the maximal variation of contents is typical of bornite from the Logatchev-1 field. The content of major (formula-forming) elements in this mineral is as follows (wt %): Cu 53.05–65.21, Fe 10.36–15.12, and S 23.79–32.15. This composition is comparable to the reference data (wt %): Cu 52–65, Fe 8–18, and S 20–27 (*Mineraly…*, 1960). The compositional variation given in Table 7 for the pink and orange varieties of bornite is similar to those presented in the literature for bornites from continental deposits (Table 8).

When recalculated to the theoretical composition of bornite Cu_5FeS_4, analyses of its varieties generally yield nonstoichiometric formulas. Our and literature data indicate that maximal deviations from the theore-

Table 7. Chemical composition of bornite from the Logatchev-1, Logatchev-2, and Rainbow fields (based on microprobe data)

Variety (number of analyses)	Content, wt %				Formula (based on 10 atoms)	Cu/Fe	Me/S
	Cu	Fe	S	Total			
Logatchev-1							
Pink (4)	64.46 – 65.21 / 64.71	10.60 – 11.08 / 10.89	23.79 – 24.87 / 24.11	99.22 – 100.55 / 99.71	$Cu_{5.18}Fe_{0.99}S_{3.83}$	5.23	1.61
Normal (15)	61.74 – 63.74 / 62.56	10.36 – 12.43 / 11.32	23.94 – 26.22 / 25.36	99.12 – 100.74 / 99.24	$Cu_{4.98}Fe_{1.02}S_{4.00}$	4.88	1.50
Orange (7)	57.06 – 61.51 / 60.26	11.63 – 14.20 / 12.42	25.78 – 28.44 / 26.50	96.95 – 100.46 / 99.18	$Cu_{4.75}Fe_{1.11}S_{4.14}$	4.23	1.42
Orange (phase A) (7)	54.09 – 55.03 / 54.62	14.19 – 15.12 / 14.64	30.04 – 30.74 / 30.37	99.41 – 100.34 / 99.87*	$Cu_{9.97}(Fe_{3.04}Au_{0.01}Hg_{0.01})_{3.06}S_{10.98}$ [2]*	3.26	1.19
Orange (phase B) (7)	53.05 – 54.60 / 53.80	12.82 – 13.52 / 13.20	31.94 – 32.15 / 32.10	98.38 – 101.00 / 99.10	$Cu_{10.97}Fe_{3.06}S_{12.97}$ [3]*	3.58	1.08
Logatchev-2							
Orange (4)	59.81 – 60.04 / 59.92	11.56 – 11.88 / 11.72	27.34 – 28.20 / 27.77	99.61 – 100.30 / 99.41	$Cu_{4.67}Fe_{1.04}S_{4.29}$	4.49	1.33
Rainbow							
Pink (5)	65.94 – 67.77 / 66.72	8.86 – 9.88 / 9.59	24.78 – 25.59 / 25.21	101.39 – 102.00 / 101.63	$Cu_{5.23}Fe_{0.85}S_{3.91}$	6.15	1.55
Normal (5)	62.98 – 64.69 / 63.70	10.78 – 12.00 / 11.31	25.13 – 26.50 / 25.60	100.13 – 101.38 / 100.85	$Cu_{4.96}Fe_{1.03}S_{4.00}$	4.82	1.50
Orange (4)	57.70 – 61.58 / 59.49	13.05 – 14.51 / 13.89	26.41 – 28.10 / 27.00	98.84 – 101.70 / 100.66	$Cu_{4.61}Fe_{1.22}S_{4.5}$	3.78	1.40
Theoretical compositions							
Normal bornite	63.33	11.12	25.55	100	$Cu^{+}_{5}Fe^{3+}S_4$	5	1.5
Orange (phase A)	54.99	14.50	30.51	100	$(Cu^{+}, Cu^{++})_{10}Fe_3S_{11}$	3.33	1.18
Orange (phase B)	54.47	13.05	32.48	100	$(Cu^{+}, Cu^{++})_{11}Fe_3S_{13}$	3.67	1.08

Note: The numerator and denominator show the variation range and average value, respectively. * Au 0.05–0.22 (average 0.13), Hg 0–0.34 (average 0.11); [2]* recalculated for 24 atoms in the formula; [3]* recalculated for 27 atoms in the formula.

Table 8. Variation range of element contents in bornites from continental deposits (based on literature data)

Variety	Content, wt %			Total	Deposit	Data source
	Cu	Fe	S			
Pink	64.6–66.7	10.44–10.89	23.4–26.01	98.98–100.79	Dzhezkazgan	Satpaeva and Polkanova, 1978
Orange	56.86–59.44	11.18–12.00	27.4–28.84	96.30–100.16		
Orange	53.65–59.48	12.72–14.18	25.50–32.09	99.94–100.99	Lubin	Large *et al.,* 1995

tical formula are observed in the orange bornite. When recalculated to four S atoms, average formula of the orange bornite from the Logatchev-1 field varies from $Cu_{4.6}FeS_4$ to $Cu_{3.4}FeS_4$. The respective formula of bornite from the Lubin Mine (Poland) ranges from $Cu_{4.5}FeS_4$ to $Cu_{3.5}FeS_4$ (Large *et al.*, 1995). If we neglect minor variations in the Fe content, the average formula of the orange bornite can be written as $Cu_{5-x}FeS_{4+x}$, where x varies from 0.04–0.16 (Logatchev-1) to 0.05–0.15 (Lubin Mine).

In ores of the Logatchev-1 field, we have found two distinct stoichiometric phases of orange bornite with $x > 1.5$—$(Cu^+,Cu^{2+})_{10}Fe_3S_{11}$ and $(Cu^+,Cu^{2+})_{11}Fe_3S_{13}$—named phases A and B, respectively. When the Cu content is decreased to retain the balance of charges, a part of this element is obviously oxidized to the bivalent state. The two phases are well developed in the assemblage mentioned above in outer zones of chalcopyrite chimneys. Phase A (mainly, lamellae in the covellite matrix of exsolution structures) has a noticeable anisotropy (from bluish gray to reddish color) and very weak bireflection. In contrast, the homogenous phase B is slightly darker and nearly isotropic. It is worth noting that these phases are compositionally closer to idaite $Cu_{3.4}FeS_4$ than to the ideal bornite. This is particular well observed in the Cu–Fe–S diagram (Fig. 4), where the data points are located on the tie line connecting data points of ideal compositions of bornite Cu_5FeS_4 and idaite Cu_3FeS_4. Data points of phases A and B in the tie line terminate the bornite composition interval with the lowest Cu and the highest S contents; i.e., their composition is closest to the theoretical idaite. Thus, the bornite–idaite boundary becomes very indefinite.

Three bornite modifications found in the Rainbow field are characterized by a lesser compositional variation (wt %): Cu 57.70–67.77, Fe 8.86–14.51, and S 24.78–28.10. In contrast to the Logatchev-1 bornite, in which Cu and S variations (12.16 and 8.36 wt %, respectively) exceed the Fe variation (4.76 wt %), the Rainbow variety shows an inverse relationship between Fe and S (5.65 and 1.69 wt %, respectively), although the maximal variation range is retained for Cu (10.07 wt %). This may indicate some differences in crystallochemical features of bornite in the two fields. Like in the Logatchev-2 field, orange bornite is less developed in the Rainbow field. Moreover, phases A and B are absent here.

Thus, the maximal compositional variation of bornite is observed in the Logatchev-1 field. Under continental conditions, analogous bornite composition range has been recorded for low-temperature sulfides in cupriferous shales in Poland. The variations are partially accompanied by the decomposition of newly formed products into covellite and chalcopyrite, probably, owing to the leaching of Cu under supergene conditions at approximately 40°C (Large *et al.*, 1995). The similarity described above indicates an obvious supergene nature of phases A and B in submarine ores of the Logatchev-1 field. This is also suggested by their confinement to fissures in the outer wall of chimneys.

Cu–S System. Minerals of this system have generally nonstoichiometric composition. They represent the youngest ore association in the studied hydrothermal fields and can be subdivided into two groups. The first group (Cu-rich sulfides of the chalcocite–digenite series) includes chalcocite, djurleite, roxbyite, digenite, and anilite (Cu/S varies from 2 to 1.75). The second group (Cu-poor sulfides of the djurleite–covellite series) includes geerite, spionkopite, jarrowite, and covellite (Cu/S varies from 1.6 to 1). Copper sulfides (except the dark blue covellite) have a gray color with bluish tint in the reflected light. The diversity of nonstoichiometric minerals in the Cu–S system is related to the fact that even a negligible deviation of copper sulfide from the stoichiometric composition is followed by the structural rearrangement of their crystalline lattice. Generally, they make up thin two-phase or polymineral blends developed after all older sulfides with the formation of patchy-reticular, colloform, stringer, rimmed, and cellular types of replacement textures (Fig. 6). The microprobe analysis was supplemented with the X-ray phase analysis to identify the minerals.

The studied hydrothermal fields significantly differ in terms of the amount of copper sulfides, their composition, and distribution pattern (Table 2, Fig. 7). In the Logatchev-1 field, they are most abundant and represented by nearly the whole spectrum ranging from chalcocite to covellite: Cu-rich sulfides (djurleite and anilite–djurleite series) prevail; chalcocite is observed as relicts in nonstoichiometric minerals; and digenite is found in decomposition products of the digenite–bornite solid solution (Gablina *et al.*, 2000).

Results of the microprobe analysis showed that roxbyite is also present in the studied objects. This mineral was discovered in the stratiform Olympic Dam Cu–U

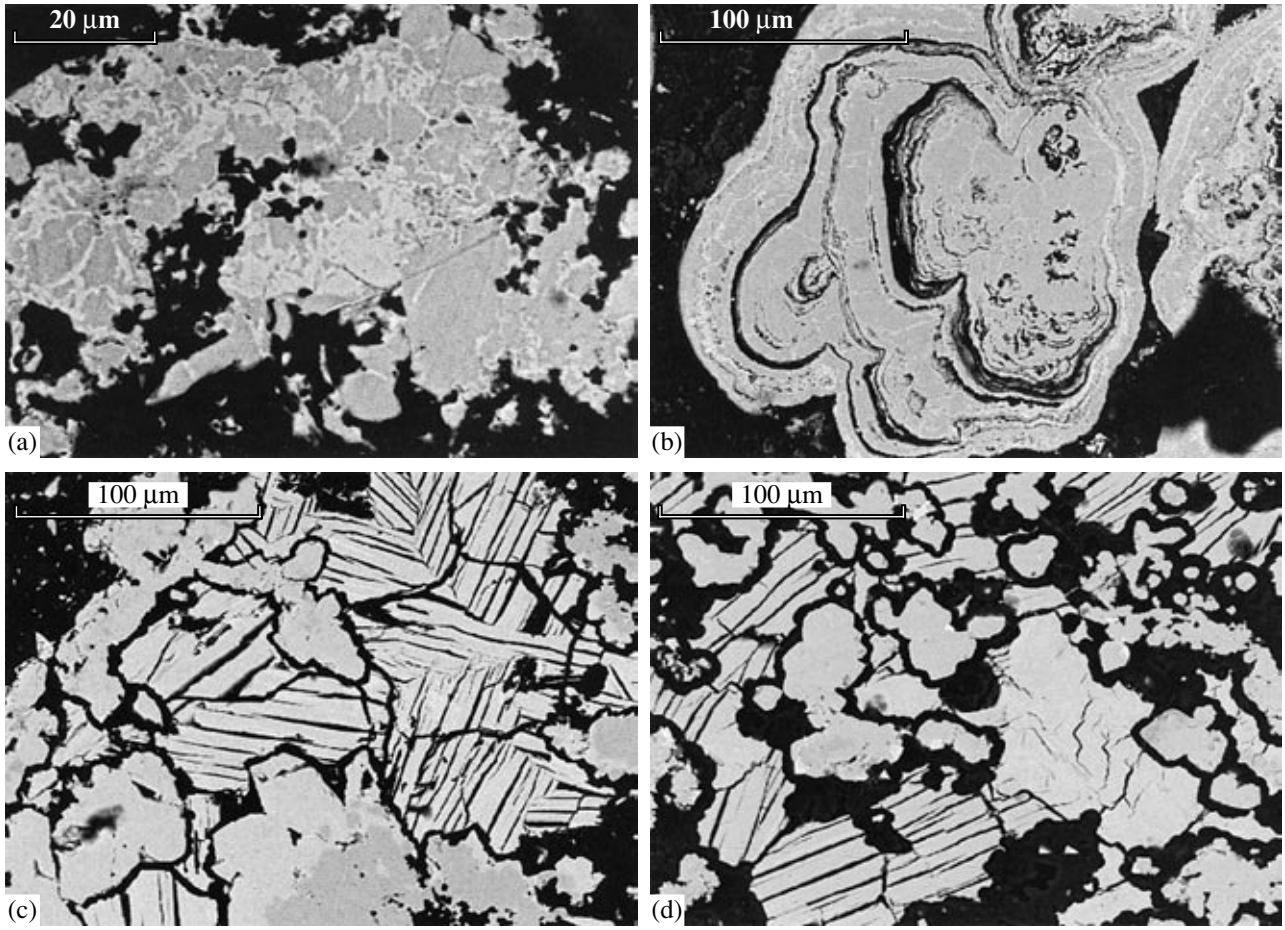

Fig. 6. Back-scattered electron images of copper sulfide segregations. Polished sections. (a) Net-textured replacement of sphalerite (gray) by geerite (light gray) (Rainbow field). (b) Colloform structure of chalcopyrite (gray) replacement by fine-grained blend of copper sulfides (light gray). (c) Aggregates of lamellar covellite (with cleavage) and sphalerite crystals with relicts of chalcopyrite (dark gray spots in the lower part). One can see fine pale spionkopite lamellae at a high magnification. Dark spot is opal. (d) Replacement of spionkopite (light gray grain with sinuous fissures at the center) by lamellar covellite. Dark tiny relicts in the spionkopite are early covellite; gray tiny rhombohedral crystals and their intergrowths are sphalerite; black spot is opal. Figs. 6b–6d are related to Logatchev-2.

deposit (Australia) as a mineral with composition matching the formula $Cu_{1.72–1.82}S$, which is similar to that of digenite. However, roxbyite has a monoclinic structure with hexagonal (very tight) packing of S atoms and a slightly lower stability temperature (65°–70°C) (Mumme *et al.*, 1988). In diffractograms, this mineral shows the following reflection peaks: 3.35, 3.00, 2.630, 2.374, 1.938, 1.861, and 1.678. In the Logatchev-1 field, roxbyite makes up pesudomorphs after hexagonal chalcocite crystallites on the outer wall of a chimney at Station 12. The XRD analysis using a Gandolfi camera revealed that the studied roxbyite is almost identical to the Australian counterpart with maximal peaks at 3.348, 3.003, 2.629, 2.389, 1.948, 1.863, and 1.675. Additional reflections and intensification of some lines suggest the presence of djurleite and anilite in the studied sample. Based on SEM data, the composition of roxbyite crystal corresponds to formula $Cu_{1.86}S$. The high Cu content is probably related to the presence of djurleite. Cu-poor minerals of the djurleite–covellite series are developed after both Fe–Zn sulfides and Cu-rich sulfides of the chalcocite–digenite series.

Copper sulfides are subordinate in the Logatchev-2 and Rainbow fields.

The Rainbow field contains both Cu-rich and Cu-poor modifications (Table 2, Fig. 7). The Cu-rich minerals of the chalcocite–digenite series (ordinary chalcocite associated with its tetragonal modification, djurleite, and/or digenite) have been recorded together with bornite at the periphery of active sulfide chimneys. Near the contact with bornite, copper sulfides have a pinky tint in the reflected light because of the formation of fine blend with bornite. It should be emphasized that distinct boundaries are absent between the Cu-rich sulfides and bornite, probably, due to the formation of a transitional zone of solid solutions.

The majority of sulfide samples from the Rainbow field are dominated by Cu-poor sulfides of the geerite–

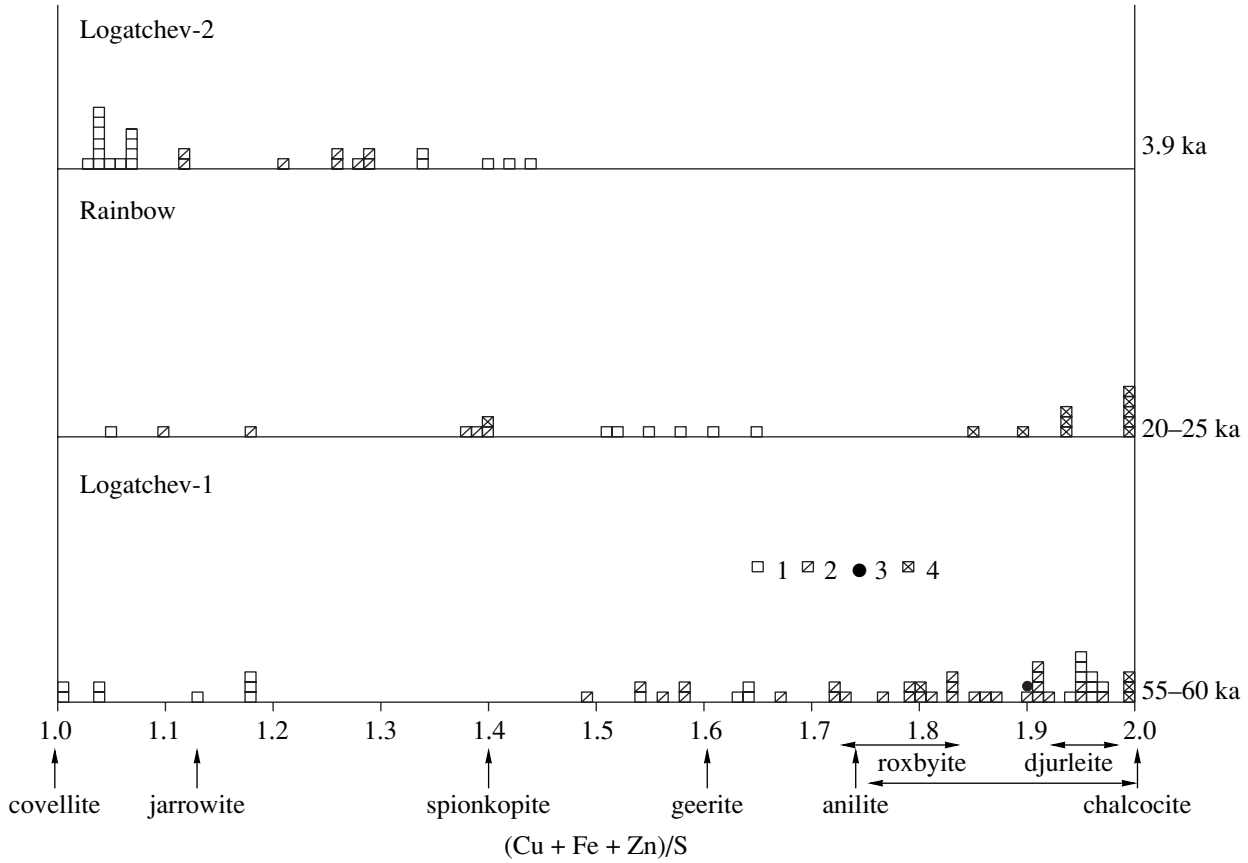

Fig. 7. Composition of copper sulfides in ores of the Logatchev-1, Logatchev-2, and Rainbow hydrothermal fields. (1–3) Based on microprobe and XRD data: (1) minerals; (2) blends; (3) average composition of digenite in digenite–bornite exsolution products; (4) minerals (based on XRD data). The column height corresponds to the number of samples.

covellite series (geerite, covellite, and polymineral blends including spionkopite and occasional geerite). They often make up a coating on sphalerite and chalcopyrite crystals on chimney walls. The copper sulfides are also observed as relatively large (up to 0.3–0.8 mm) aggregates developed after chalcopyrite and sphalerite on the inner wall of chimneys (Fig. 6a). Geerite rarely makes up homogenous segregations. Generally, this mineral contains tiny covellite inclusions that are responsible for distortion of the real geerite composition in microprobe analyses. As is evident from Fig. 7, the Cu/S ration in geerite varies from 1.51 to 1.65 (average 1.55). It always includes some Fe and/or Zn. When the trace element contents are recalculated to ideal formulas of sphalerite or chalcopyrite, the Cu/S ratio in geerite approaches the theoretical value. In some cases, covellite is observed as large lamellas (10 μm or more). Its composition varies from $Cu_{1.05}S$ to $Cu_{1.18}S$, probably, owing to the presence of a very fine admixture of Cu-rich minerals.

Of particular interest is the discovery of a high-temperature metastable modification Cu_2S ("tetragonal chalcocite") in samples 4393-2 and 4412-6 (Gablina *et al.*, 2004). This mineral was established in the high-temperature synthesis of copper sulfides and regarded as a metastable phase. According to Djurle (1958) and other researchers, this phase is produced during polymorphous transitions of the high-temperature hexagonal chalcocite into the cubic modification (at 430–450°C) or the monoclinic modification (at 102°C). The tetragonal modification is indiscernible from the ordinary chalcocite in the reflected light and can only be identified based on XRD analysis. The mineral is gradually transformed into different polymorphs. Interestingly, the tetragonal chalcocite found in the Rainbow field is confined to walls of an active vent, i.e., the highest-temperature sectors of the hydrothermal mound.

The Logatchev-2 field only contains Cu-poor sulfides of the geerite–covellite series and, thus, significantly differs from the Logatchev-1 and Rainbow fields (Fig. 7). Covellite, the major mineral, is developed as lamellar (up to 80 μm along the long axis) aggregates between sphalerite crystals (Figs. 6c, 6d). At higher magnifications, one can see that the covellite includes lamellae of Cu-rich minerals (generally, spionkopite) that distort the covellite composition. Polymineral blends of spionkopite with covellite, jarrowite, and occasional geerite are metasomatically developed after grain boundaries or different zones in colloform bornite, chalcopyrite, and sphalerite.

Table 9. Coefficients of correlation between element concentrations in pentlandites from the Rainbow field

	Ni	Co	Fe	Cu	S
Ni	1	–0.92	0.43	0.06	0.36
Co		1	–0.68	–0.15	–0.24
Fe			1	–0.21	–0.18
Cu				1	–0.44
S					1

Note: Based on 30 analyses (95% confidence interval). Coefficients of correlation exceeding 0.25 (in absolute value) are significant.

Thus, all of the studied hydrothermal fields contain Cu-poor sulfides of the geerite–covellite series. They are developed both near active sources and in extinct hydrothermal areas. The Cu-rich sulfides (chalcocite–digenite series) are confined to the Logatchev-1 and Rainbow fields with active modern hydrothermal activity. Djurleite and anilite prevail in the oldest Logatchev-1 field characterized by the longest hydrothermal activity. In the young and most active Rainbow field, anilite is absent in the Cu-rich sulfide assemblage, but the tetragonal Cu_2S is present. The tetragonal phase seems to be a primary hydrothermal mineral retained under specific thermodynamic conditions of the functioning of deep-water thermal sources. In inactive sectors of the older Logatchev-1 field, chalcocite relicts are commonly associated with its oxidation products (djurleite, roxbyite, anilite, geerite, spionkopite, jarrowite, and covellite).

Co–Ni–Fe–S System. Co-pentlandite, first representative of the Co–Ni–Fe–S system in oceanic ores, was discovered in the Logatchev-1 field and considered a typomorphic mineral of hydrothermal mounds related to ultramafic rocks (Mozgova *et al.*, 1996). This was confirmed by finds of this mineralization in the Rainbow field (Bogdanov *et al.*, 2002; Bortnikov *et al.*, 2001; Mozgova *et al.*, 2005; Vikent'ev, 2001). This mineral has not been found in the Logatchev-2 field.

In the Rainbow field, Co–Ni mineralization has been recorded in sulfide chimneys of active smokers in the new "smoke zone" (Borodaev *et al.*, 2004b). In contrast to the Logatchev-1 field, where Co-pentlandite is confined to bornite stringers that crosscut compact chalcopyrite ores and, in turn, are crosscut by chalcocite veinlets, the Rainbow field is characterized by a wide range of Co–Ni sulfides (millerite, pentlandite, and Co-pentlandite) that are developed in copper chimneys at some distance from the vent. Small grains (up to 10–15 μm) are observed near the chalcopyrite–bornite transition zone and in the marginal copper sulfide zone. The grains are developed as separate phenocrysts and fine vermicular segregations in contact-line zones. They are also often confined to bornite stringers in chalcopyrite.

The absence of Co–Ni minerals in the central parts of chimneys may be caused by the prolonged delivery of hot fluids that provoked sublimation of Co and Ni toward the vent ("zonal cleaning"). If these elements encountered seawater seeps, they could form Co–Ni minerals on chimney walls. The zonal cleaning in sulfide chimneys of black smokers, a phenomenon responsible for the zonal distribution and concentration of Co in marginal zones, was revealed by the neutron activation beta-autography (Zhmodik *et al.*, 2001).

The chemical composition of millerite is nearly constant and close to the theoretical NiS. The pentlandite composition shows the following variation (wt %): Ni 18.28–37.05, Co 13.17–35.67, Fe 9.51–17.52, Cu 1.38–8.02, and S 30.37–34.71. Some analyses show the presence of Ag (up to 0.46 wt %) and Au (up to 0.13 wt %). Recalculation of these analyses into the general formula of minerals of the pentlandite group Me_9S_8 (17 atoms) revealed that the (Ni + Fe + Cu): Co ratio generally exceeds unity (1.22–4.13). Co prevails and the ratio becomes less than unity (0.89 and 0.90) only in two analyses. Based on MMA recommendations suggesting the 50%-boundary for the identification of mineral species in isomorphic series (Nickel, 1992) and the isomorphism scheme accepted for pentlandite $Co_9S_8 \rightleftarrows Ni_{4.5}Fe_{4.5}S_8$ (Rajamani and Prewitt, 1973; Vaughan and Craig, 1978; and others), the analyzed mineral corresponds to pentlandite (28 grains) or Co-pentlandite (2 grains). Statistical processing of pentlandites from the Rainbow field (Table 9) revealed a high negative Co–Ni correlation and a significant (but weaker) negative Co–Fe correlation. These data differ from those previously obtained for Co-pentlandite (Co 42.9–53.9, Ni 8.4–12.4, Fe 3.4–5.5, Cu 0.7–9.4, and S 31.6–32.9 wt %) from the Logatchev-1 field characterized by a negative Co–Fe correlation and the absence of Co–Ni correlation (Mozgova *et al.*, 1996).

One can get additional information concerning Co–Ni and Co–Fe correlations from plots showing results of the recalculation of analyses (Fig. 8). In the Rainbow field, Ni shows an inverse correlation with Co, but this relation is complicated by small fluctuations of the Co curve suggesting an inverse correlation with the (Fe + Cu) content (Fig. 8a). In the plot based on data related to Co-pentlandite in the Logatchev-1 field, one can only observe the negative Co–(Fe + Cu) correlation, while the Ni behavior is inert (Fig. 8b).

The relations described above are reflected in the distribution of data points in the Co–Ni–(Fe + Cu) diagram. Data points of Rainbow pentlandites make up a band parallel to the Co–Ni side, while Co-pentlandites from the Logatchev-1 field extend parallel to the Co–(Fe + Cu) side (Fig. 9).

These relations, evidently, testify to different styles of isomorphic replacements in the minerals. In the Rainbow pentlandite, isomorphism scheme Co $\rightleftarrows$ Ni plays the major role, while isomorphism scheme Co $\rightleftarrows$ (Fe + Cu) is subordinate. In the Logatchev-1

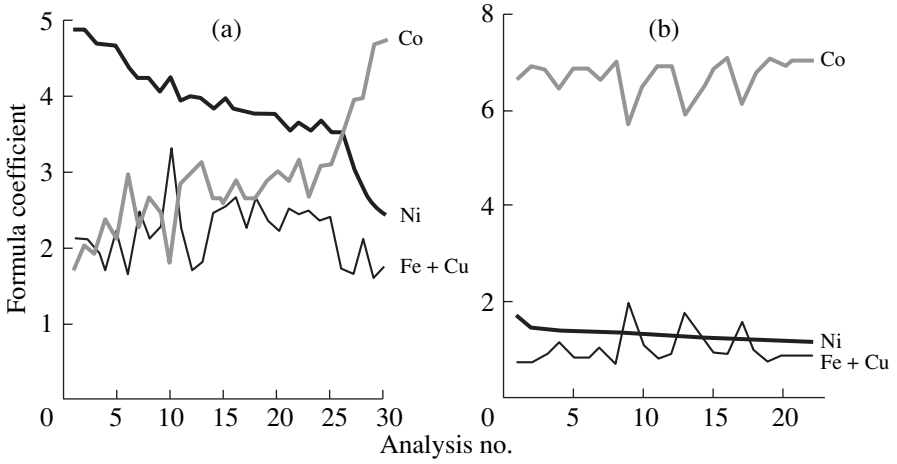

Fig. 8. Relationship of major elements in pentlandite and Co-pentlandite grains. (a) Rainbow; (b) Logatchev-1.

field, the predominant isomorphism scheme is Co ⇄ (Fe + Cu). The existence of two styles of isomorphism in the oceanic pentlandite is consistent with trends of isomorphic replacements in the continental pentlandite (Riley, 1977).

Mineral assemblages with Co–Ni sulfides are nearly similar in ores of the Logatchev-1 and Rainbow fields (chalcopyrite, bornite, and copper sulfides). The assemblage is supplemented with isocubanite in the Logatchev-1 field and with isocubanite-type phase Y in the Rainbow copper chimney. However, the Co content is as much as 64–79 at % in the Logatchev-1 Co-pentlandite and only 20–53 at % in the Rainbow pentlandite. The first interval matches the interval for the continental pentlandite associated with cubanite, whereas the second interval matches the value reported for the mineral associated with pyrrhotite, pyrite, and chalcopyrite. We suppose that discrepancies detected in the pentlandite composition are related to differences in age, activity, and maturity of the Logatchev-1 and Rainbow fields. Sulfides of the Logatchev-1 are more mature and closer to continental ores in composition. Therefore, the dependence of pentlandite from the mineral assemblage in this field is rather similar to trends established for the continental Co–Ni associations. Deviations from these trends in the Rainbow field, probably, testify to an unstable active evolution of young sulfide chimneys.

SPECIFIC FEATURES OF TEXTURAL–STRUCTURAL RELATIONSHIPS IN ORE MINERALS

The studied sulfide ores are characterized by a wide development of diverse exsolution structures that can make it possible to solve genetic issues based on the study of temporal transformations minerals. The exsolution structures are most widespread in compounds of the Cu–Fe–S system due to the diffusion of components in the course of iss and bss exsolution (Brett, 1964; Sugaki *et al.*, 1975; and others). Both iss and bss exsolution structures are observed in oceanic sulfide ores (Mozgova *et al.*, 2002a).

Exsolution structures of phase iss (isocubanite solid solution) are widespread in oceanic ores, including ores in the Logatchev-1, Logatchev-2, and Rainbow fields. These structures differ in morphology, quantitative proportions of decomposition products, and their chemical composition.

Latticed and lamellar structures and their combination are most widespread. Their quantitative relationships in newly formed phases vary from rare fine lamellae in the matrix to large lamellae in local aggregates. In some cases, both types of lamella are approximately equally developed. The lamella are up to 120 μm long and *n* to 10–15 μm wide. One can see indications of

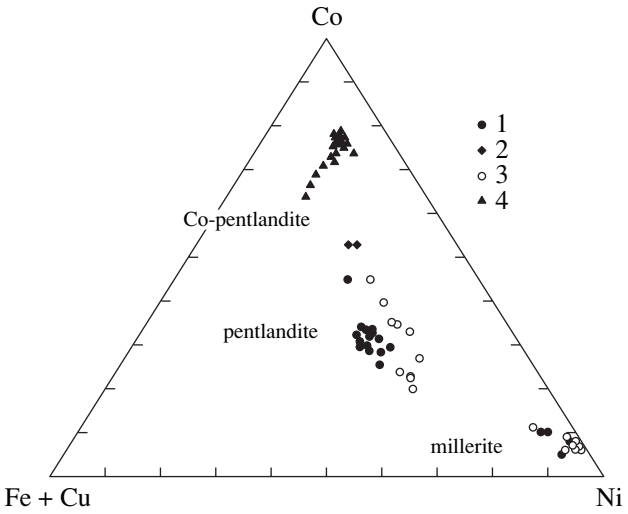

Fig. 9. The Co–Ni–(Fe + Cu) diagram for Co–Ni minerals in submarine sulfides. (1–3) Rainbow: (1) pentlandite, (2) Co-pentlandite, (3) pentlandite (Bogdanov *et al.*, 2002); (4) Logatchev-1, Co-pentlandite (Mozgova *et al.*, 1996).

multistage decomposition: matrix sandwiched between large lamellae is often complicated by exsolution structures of II or even III order, and the whole structure is sometimes rimmed with homogenous chalcopyrite. In terms of chemical composition of exsolution products, one can identify two types of structures. Lamellae in the isocubanite matrix are composed of phases X and Y in the first and second types, respectively. In both cases, the lamellae are Cu-enriched and paler in the reflected light relative to the matrix. The second type is less common. Since the compositional difference is less contrasting in lamellae of the second type, they are less discernible under a microscope. The alternation of different phases is distinctly seen in linear scanning profiles across the exsolution structures (Figs. 10a, 10b). They were probably formed at sufficiently high temperatures, because the matrix is composed of isocubanite. According to experimental data (Yund and Kullerud, 1966), the temperature of isocubanite inversion into the ordinary tetragonal cubanite is 252°C.

Comparative analysis of data revealed some differences in the distribution and specific features of exsolution structures in the studied objects.

Both chemical types of structure are developed in the Logatchev-1 and Logatchev-2 fields. However, the structures are more diverse in morphology and more contrasting in the composition of newly formed phases. In the Logatchev-1 field, the contrast expressed as difference in the Cu content (at %) between lamellas and matrix is 8.56 for phase X lamellas and 4.96 for phase Y lamellas. In ores of the Logatchev-2 field, the contrast is considerably lower (5.17 and 2.78, respectively). In the Rainbow field, such structures are associated with sphalerite and they are less discernible. Therefore, we could not analyze the exsolution products. Results of the areal scanning indicate that homogenous isocubanite associated with iron disulfides in the Rainbow field is depleted in Cu (14.67 at. %), relative to the primary (undecomposed) isocubanite (Cu 15.67 at. %) in samples from the Logatchev-1 field.

In the Logatchev-1 field, exsolution products demonstrate an inverse correlation with the composition of ore associations. For example, chalcopyrite lamellas and isocubanite matrix in exsolution structures of the copper zone turned out to be enriched in Fe, relative to their counterparts in the Fe-rich zone (Mozgova *et al.*, 1999).

Exsolution structures of the bornite solid solution (bss). It is known from experiments with the Cu–Fe–S system that phase bss, together with phase iss, predominates in the central part of the Cu–Fe–S system at temperature ≤700°C (Yund and Kullerud, 1966). As was shown above, bornites (including the orange variety) in the studied ores are also characterized by a wide range of S and Cu contents. The bss exsolution structures are well manifested in a small chalcopyrite chimney of the Logatchev-1 field. The sample for analysis was kindly placed at our disposal by I. Poroshina.

Around fissures extending from the periphery of the chimney to its center, one can see that chalcopyrite is replaced by younger minerals, probably, related to reaction with the penetrating seawater (Fig. 11). The fissures are surrounded by a thin rim of copper sulfide blend with distinct covellite segregations. Its composition (Cu 67.68, Fe 0.65, and S 32.06 wt %) corresponds to formula $Cu_{1.06}Fe_{0.06}S$. The zone between the rim and chalcopyrite is filled with irregular orange bornite that is mostly decomposed with the formation of complex (two-stage) exsolution structures. The matrix is dominated by a coarse network of large lamellae (up to 10 μm wide) that is composed of another network of thin lamellae oriented perpendicularly to the first network (Fig. 12). The quantitative proportion of exsolution products is variable. The orange bornite aggregate corrodes chalcopyrite and includes its relicts.

Scanning across large lamellae and microprobe analyses of separate points demonstrated that the studied lamellae compositionally correspond to phase B $(Cu^{+},Cu^{++})_{11}Fe_3S_{13}$, while the orange bornite corresponds to phase A $(Cu^{+},Cu^{2+})_{10}Fe_3S_{11}$. The bulk composition of the matrix corresponds to covellite (wt %): Cu 66.58, Fe 3.79, S 30.44, and total 100.81. Its chemical formula can be written as $Cu_{1.10}Fe_{0.07}S$. Unfortunately, we could not analyze the lamellae because of their tiny dimensions.

Chalcopyrite–sphalerite myrmekitic structures are observed in zonal chimneys of the Logatchev-2 field. They are mainly composed of sphalerite in the outer zone and chalcopyrite in the inner zone near the vent (Figs. 13a, 13b). Intergrowths of these minerals are developed in the contact zone. When passing from the Zn-rich zone to the Cu-rich zone toward the vent, the sphalerite–chalcopyrite assemblage (with the specific structure of mutual boundaries dominated by sphalerite) gives way to the chalcopyrite with sphalerite lamellae. Similar structures are also observed in chimneys with an inverse arrangement of zones.

In experimental mineralogy, such intergrowths are regarded as exsolution structures (Amcoff, 1981; Brett, 1964; and others). Structural relationships of chalcopyrite and sphalerite in oceanic ores described above may be attributed to the decomposition of metastable solid solutions.

Native gold and its intergrowths with arsenic. As was mentioned in the introduction, all the studied hydrothermal fields are auriferous objects, the Logatchev-1 and Logatchev-2 fields being characterized by the highest Au contents (Table 1). This trend is also reflected in the amount of native gold segregations.

According to (Lazareva *et al.*, 1998), the macroscopic gold is mainly found in copper ores of the Logatchev-1 field. Fine-dispersed gold particles (1–1.5 μm) are found as syngenetic products in the early chalcopyrite. Slightly larger grains (1.5–2 μm) are observed in the Fe-sphalerite (often, in pores within

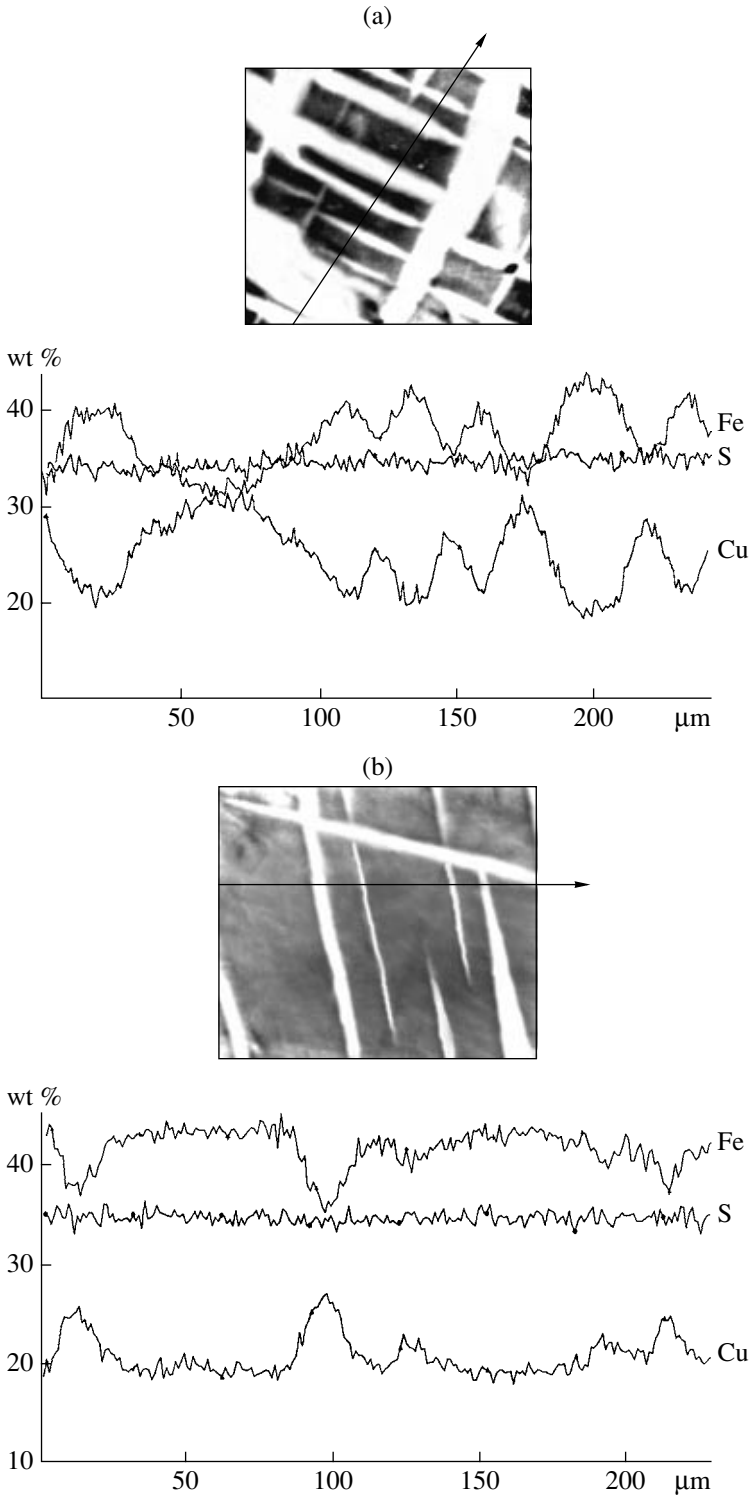

Fig. 10. Iss exsolution structures with various compositions of lamellae (pale). Matrix (gray) is composed of isocubanite (Logatchev-1). Polished sections; back-scattered electron images and linear scanning plots (scanning direction and extent are shown by arrow); width of photomicrograph is 250 μm. (a) lamellae of phase X; (b) lamellae of phase Y.

the mineral). Native gold and silver typically occur in aragonite in the chalcopyrite–chalcocite–aragonite breccia. The gold flakes are usually 0.3–6 μm in size (rarely, up to 30–40 μm). The grains are generally rounded. Locally, one can see irregular grains inheriting the shape of cracks and pores.

High average Au contents in ores of the Logatchev-2 field reflect the abundance of large segregations of

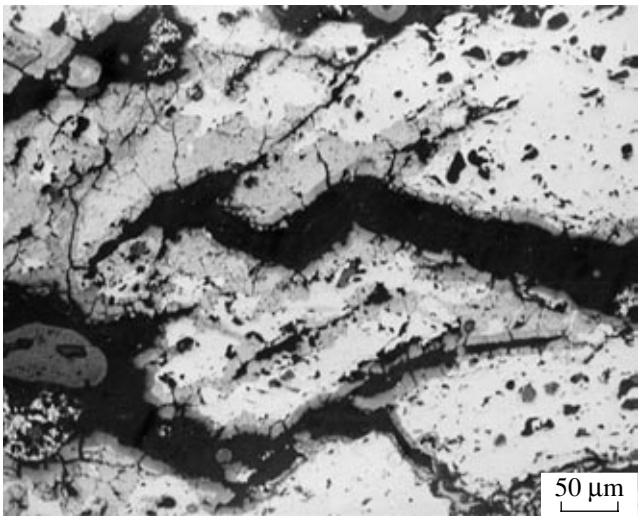

Fig. 11. Late mineralization developed after chalcopyrite along crosscutting fissures at the margin of a small copper chimney (Logatchev-1). Polished section, reflected light. Chalcopyrite (white) is replaced by orange bornite and bornite–covellite blend (gray) with exsolution structure (indistinct). A thin rim of copper sulfides (dark gray) is developed along the fissures (black).

native gold (up to 5 μm across) that are primarily confined to siliceous minerals at the contact with sphalerite and chalcopyrite (Lein *et al.*, 2001). The gold grains are often rounded, but subhedral grains with square sections are also found in some places.

In the Logatchev-2 field, we have discovered (for the first time in oceanic ores) zonal intergrowths of gold with native arsenic in the siliceous substrate (Mozgova *et al.*, 2002a). The intergrowths are composed of gold in the core and native arsenic (often with outer crystallographic outlines) in the rim (Fig. 14). Such segregations are scattered (sometimes, as clusters and chains) in silica. When the gold flake occurs at the contact and partially within sphalerite grains, the arsenic rim only envelops their silica-facing side and is absent at the contact with sphalerite. Therefore, we support the opinion of Powell and Pattison (1997) based on observation of similar intergrowths in the Hemlo gold deposit (Canada), suggesting that the intergrowths are decomposition products of the high-temperature gold–arsenic alloy. These researchers believe that arsenic could completely abandon the gold core because of its microscopic dimension.

DISCUSSION

Previous investigations of sulfide ores from the Logatchev-1, Logatchev-2, and Rainbow hydrothermal fields of the MAR, which are located in ultramafic rocks in similar geostructural settings but differed in age, duration of ancient hydrothermal activity, and degree of modern hydrothermal activity, revealed a number of discrepancies in their mineralogical–geochemical features. Therefore, Lein *et al.* (2003) concluded that primary rocks do not govern the specialization of associated ores. However, factors responsible for the discrepancies remained unclear.

We scrutinized data on ores in these objects and elucidated geochemical relations of mineral assemblages with specific features of ore genesis. The available data indicate that maturity of hydrothermal mounds governs the mineralogical–geochemical discrepancies.

It is common knowledge that hydrothermal ores are formed in ocean at the front where hot (up to 400°C) acid (pH = 3.7) fluids are mixed with cold (2°C) low-alkaline (pH = 7–8) oxidative seawater (Simonov and Milosnov, 1996). It is convenient to examine the further evolution of hydrothermal ore formation on the basis of Cu–Fe–S and Cu–S systems, because these systems incorporate valence-variable elements. They show a wide composition range and rapidly respond to variations in the environment.

As soon as the minerals are formed in active smokers, they are subjected to simultaneous impact of the continuous flow of fluids and the ambient seawater heated to a certain extent by fluids. The study of young copper sulfide chimneys in the Rainbow field (Borodaev *et al.*, 2004a, 2004b) showed that the reaction of fluids with seawater produces two oppositely oriented metasomatic columns. The growth of mineral aggregates is oriented from the center to periphery in the endogenous column and from the periphery to center in the exogenous column. The role of exogenous column rises and the supergene process begins to dominate with waning of the endogenous hydrothermal process.

In an oxidative environment created by seawater, transformation of Cu–Fe sulfides begins with oxidation of the bivalent Fe and its removal, leading to the formation of Cu-rich minerals of the Cu–Fe–S system that gradually give way to copper sulfides. Thus, Cu is concentrated with decrease in the sulfide ion activity according to the following scheme (hereafter, the valence of elements in formulas is shown based on the Mössbauer data): isocubanite $Cu^{+}Fe^{2+}Fe^{3+}S_3$ ⟶ chalcopyrite $Cu^{+}Fe^{3+}S_2$ ⟶ bornite $Cu_5^{+}Fe^{3+}S_4$ (including bornite–digenite solid solutions) ⟶ minerals of the Cu–S system (mainly nonstoichiometric). With decrease of the hydrothermal flow and intensification of the impact of seawater, Cu is gradually oxidized and removed, resulting in the successive replacement of Cu-rich minerals by Cu-poor species. This scheme is consistent with supergene alterations of Cu–Fe sulfides reported from continental deposits (Constantinou, 1975; Large *et al.*, 1995; Sillitoe and Clark, 1969; and others). The Cu content decreases (correspondingly, the S content increases) in Cu–S minerals as a result of the gradual oxidation of Cu to Cu^{2+}. Such relationships are long known for nonstoichiometric copper sulfides (Belov, 1953; Eliseev *et al.*, 1964).

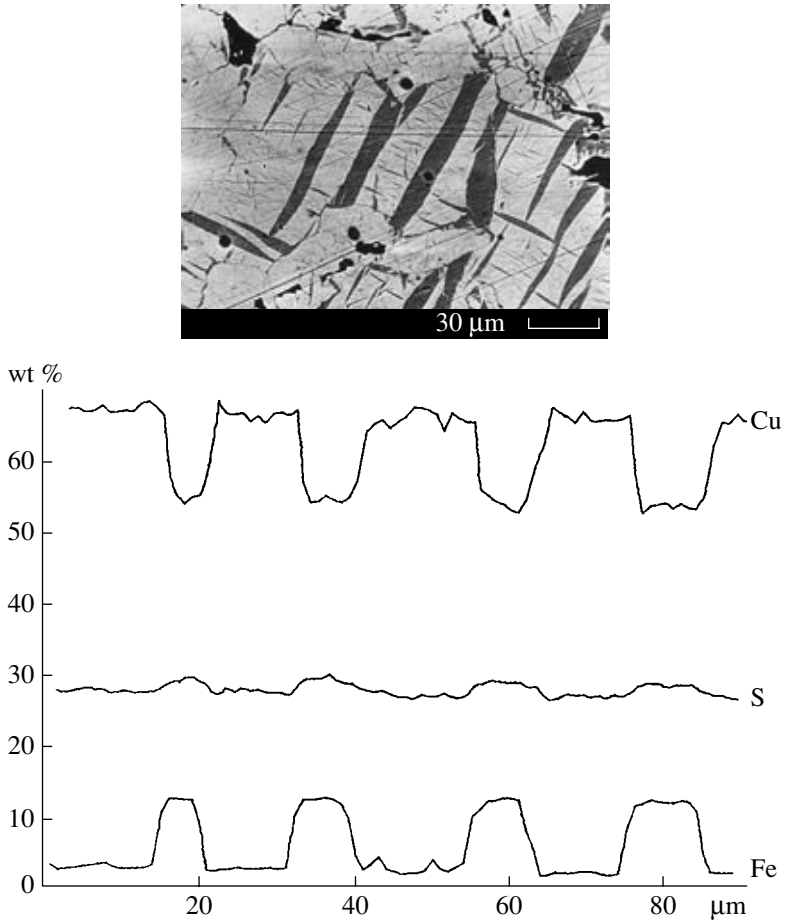

Fig. 12. Two-stage exsolution structure composed of large lamellae of phase B (orange bornite, black) in covellite matrix (pale) with thin lamellae of bornite (gray) and the curve of linear scanning perpendicular to large lamellae. Polished section, back-scattered electron image.

Solid solutions of the Cu–Fe–S system undergo substantial transformations. According to numerous experimental data (Cabri, 1973; Sugaki *et al.*, 1975; Yund and Kullerud, 1966; and others), the central part of the Cu–Fe–S system includes a wide region of solid solutions at high temperatures (600–700°C). As the temperature decreases, the region is divided into the tetragonal css and cubic iss branches. The miscibility gap occurs already at 500°C (Yund and Kullerud, 1966). It is also known from (Amcoff, 1981; Brett, 1964; and others) that exsolution structures are related to the diffusion of components in a solid medium. Duration of process is an essential factor. Obviously, the degree of structure transformation directly correlates with the duration of process.

In connection with the trend of hydrothermal sulfide formation in oceans discussed above, let us highlight the major specific features of sulfide ores and their comparative aspects.

The studied objects mainly differ in terms of the chemical specialization of ores, quantitative proportions of major minerals, compositions of some universal compound sulfides, and their structural–textural relationships. The available data suggest that the ores were altered in the course of autometasomatism and hypergenesis.

In the most long-lived and reworked Logatchev-1 ore field with a waning hydrothermal activity, ores are characterized by the copper specialization, absence of pyrrhotite, maximal morphological diversity, and abundance of multistage exsolution structures of isocubanite and bornite in a wide temperature range with the most contrast decomposition products and the maximal sizes of lamellae. Orange bornites in this hydrothermal field contain phases A and B with very high S and Fe contents and stoichiometric compositions approaching the idaite composition. One can also see the maximal development and diversity of sulfides of the Cu–S system, whereas native metals (copper and natural brass) are found in the typical supergene assemblage. The mineral assemblage of Co-pentlandite is similar to that in continental ores.

The Logatchev-2 and Rainbow fields are specialized in Cu–Zn mineralization. The short-lived and already

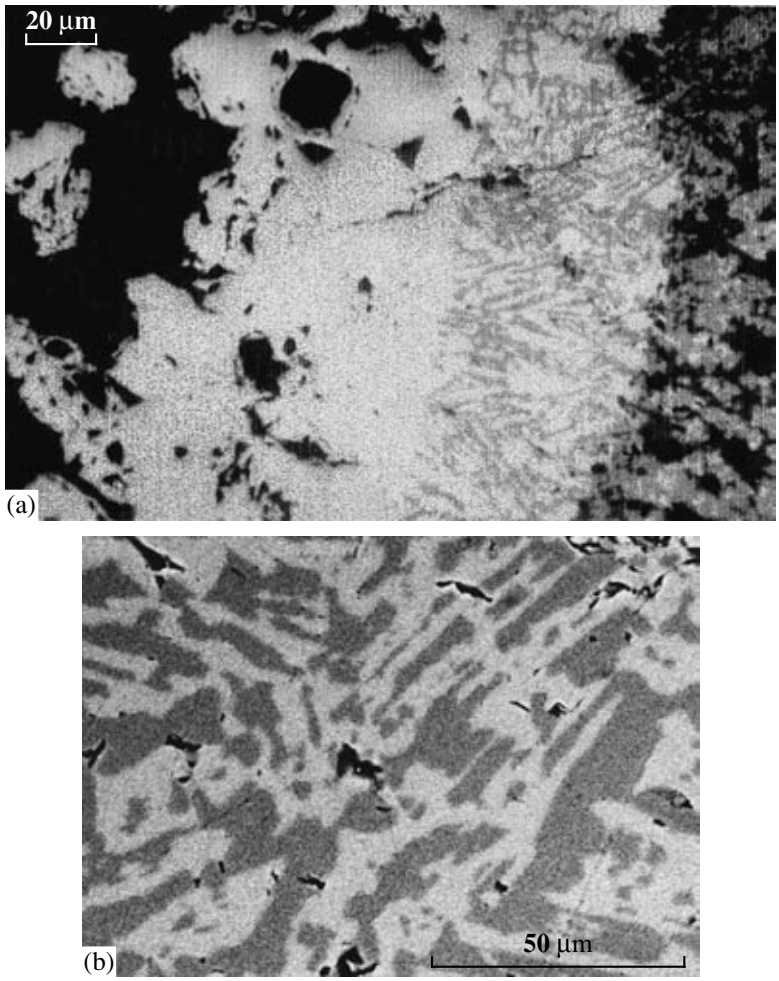

Fig. 13. Relationship of chalcopyrite and sphalerite (Logatchev-2). Polished sections. (a) Zonal distribution of intergrowths of chalcopyrite (white) and sphalerite (gray) around the conduit. Reflected light. (b) Graphic structure of intergrowths of sphalerite (pale) and chalcopyrite (dark). Back-scattered electron images.

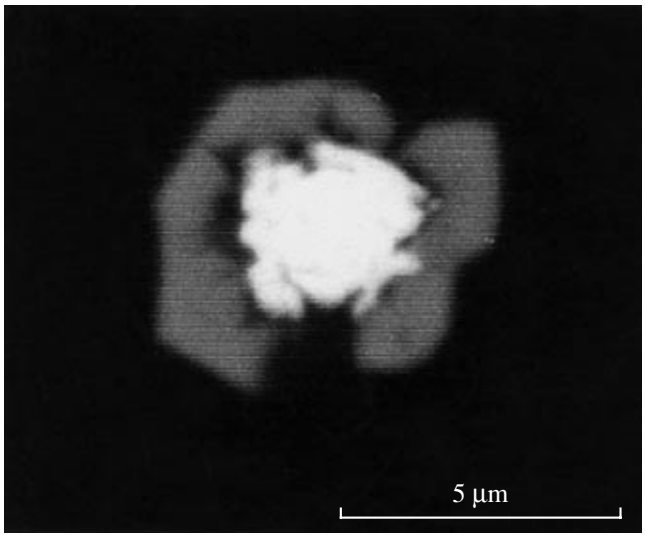

Fig. 14. Native gold grain with a rim of native arsenic crystals in silica (Logatchev-2). Polished section, back-scattered electron image.

inactive Logatchev-2 edifice is characterized by the abundance of colloform textures and intergrowths of different (sphalerite–chalcopyrite and gold–arsenic) minerals that are interpreted as exsolution structures of respective solid solutions. In these hydrothermal fields, the morphology of isocubanite exsolution structures is not so diverse and their products are less contrast. Like other native metals, the accessory gold is found among primary sulfides unaltered by supergene processes. This inference is consistent with the earlier opinion suggesting the input of Au by primary fluids together with ore components (Borodaev *et al.*, 2000). Copper sulfides are less developed (mainly minerals of the Cu-poor geerite–covellite series). In the Rainbow field marked by modern hydrothermal activity, pyrrhotite is abundant in association with homogenous isocubanite characterized by the minimal Cu content (relative to reconstructed compositions of primary isocubanite in other objects). Exsolution structures of this isocubanite are subordinate and confined to sphalerite segregations. The exsolution structures are fine-latticed and poorly

discernible under a microscope because of low contrast of phases. In ores of the Logatchev-1 and Logatchev-2 fields, phase Y is only observed as lamellae in iss exsolution structures. In ores of the Rainbow field, phase Y makes up homogenous zones in zonal copper chimneys. Here, copper sulfides are mainly developed at the chimney periphery. Walls of the active vent contain stoichiometric chalcocite and the high-temperature metastable modification of tetragonal chalcocite that has been found for the first time in oceanic ores.

Results of comparison of specific features of the studied ores with the trend of oceanic hydrothermal ore formation suggest the existence of certain indications of their genetic relation with the substrate (e.g., high Co and Ni contents in ores and the presence of accessory minerals of these elements). Discrepancies revealed in this process can be explained by the duration of the functioning and degree of activity of modern hydrothermal systems.

In conclusion, we should note that the behavior of sulfide minerals in modern hydrothermal systems provide new insights into the central part of the Cu–Fe–S system that has been the focus of attention over a long time. We have discovered the following four new natural compounds in this system: phase X $Cu_{0.9}Fe_{1.1}S_2$ (anomalous nonstoichiometric chalcopyrite corresponding to the Fe-rich end member of the css at 350°C), phase Y $Cu_{0.8}Fe_{1.2}S_2$ (anomalous Cu-isocubanite), and phases A and B with stoichiometric proportions of formula-forming elements in orange bornites with the highest S contents. In oceanic ores, we have first scrutinized the readily oxidizable (and disordered) chalcopyrite and found the rare metastable tetragonal modification of chalcocite. The investigation of the recently discovered Co–Ni mineralization in submarine ores has confirmed two models of isomorphism that were previously proposed for the continental pentlandite. This has opened new avenues for the study of this essential group of minerals.

CONCLUSION

(1) Results of the study of three hydrothermal fields (Logatchev-1, Logatchev-2, and Rainbow) related to ultramafic rocks indicate that specific features of mineral assemblages in them reflect the maturity of sulfide mounds and can serve as indicators of the degree of maturity.

(2) Copper specialization of ores in mature seamounts with the prolonged-term functioning of convective hydrothermal systems can be related to the transformation of sulfide ores under the long-term influence of the ambient seawater.

(3) Mineralogical–geochemical investigations of products of modern sulfide formation deposited on the seafloor under disequilibrium conditions provide new insights into metastable phases of the Cu–Fe–S system that has important geological implications, because minerals in this system make up many continental deposits.

ACKNOWLEDGMENTS

We are grateful to I.A. Bryzgalov, N.V. Trubkin, and O.A. Kuznetsova for help in the performance of analytical investigations, the Polar Marine Geoexploration Expedition for ore samples from the Logatchev-2 field, and Prof. V.I. Starostin for the collection of samples from the Rainbow smoke zone. We are particularly grateful to G.Yu. Butuzova for fruitful discussion of the manuscript and valuable advices.

This work was supported by the Russian Foundation for Basic Research (project no. 01-05-64679) and the Ministry of Science and Technology of the Russian Federation (project no. 3.2.2 of the Federal Program "World Ocean").

REFERENCES

Amcoff, Ö., Heating Experiments of Chalcopyrite-Pyrrhotite Ores: Studies on the Stability of the Intermediate Solid Solution, *Neues. Jahrb. Mineral. Monatsh.*, 1981, pp. 553–568.

Anthony, J.W., Bideaux, R.A., Bladh, K.W., and Nichols, M.C., *Handbook of Mineralogy. I. Elements, Sulfides, Sulfosalts*, Tuscon: Mineral Data Publ., 1990.

Belov, N.V., Some Aspects of Sulfide Crystallochemistry, *Voprosy Petrol. Mineral.*, 1953, vol. 2, pp. 7–13.

Bogdanov, Yu.A., *Gidrotermal'nye rudoproyavleniya Sredinno-Atlanticheskogo khrebta* (Hydrothermal Ore Occurrences in the Mid-Atlantic Ridge), Moscow: Nauchnyi Mir, 1997.

Bogdanov, Yu.A. and Sagalevich, A.M., *Geologicheskie issledovaniya s glubokovodnykh obitaemykh apparatov "Mir"* (Geological Surveys from Manned Submersibles "Mir"), Moscow: Nauchnyi Mir, 2002.

Bogdanov, Yu.A., Bortnikov, N.S., Vikent'ev, I.V., Gurvich, E.G., and Sagalevich, A.M., A New Type of Modern Mineral-Forming System: Black Smokers of the Hydrothermal Field at 14°45′ N, Mid-Atlantic Ridge, *Geol. Rudn. Mestorozhd.*, 1997, vol. 39, no. 1, pp. 68–90 [Geol. Ore Dep. (Engl. Transl.), 1997, vol. 39, no. 1, pp. 58–79].

Bogdanov, Yu.A., Bortnikov, N.S., Vikent'ev, I.V., Lein, A.Yu., Gurvich, E.G., Sagalevich, A.M., Simonov, V.A., Ikorskii, S.V., Stavrova, O.O., and Apollonov, V.N., Mineralogical–Geochemical Peculiarities of Hydrothermal Sulfide Ores and Fluids in the Rainbow Field Associated with Serpentinites, Mid-Atlantic Ridge (36°14′ N), *Geol. Rudn. Mestorozhd.*, 2002, vol. 44, no. 6, pp. 510–542 [Geol. Ore Dep. (Engl. Transl.), 2002, vol. 44, no. 6, pp. 444–473].

Borodaev, Yu.S., Mozgova, N.N., Stepanova, T.V., and Cherkashev, G.A., Noble Metals in the Sulfide Associations of Chimneys in the Logatchev Hydrothermal Field (Mid-Atlantic Ridge, 14°45′ N), *Vestn. Mos. Gos. Univ., Ser. 4: Geol.*, 2000, no. 3, pp. 40–49.

Borodaev, Yu.S., Mozgova, N.N., Gablina, I.F., *et al.*, Model of Formation of Black Smoker Zonal Chimneys from Active Mounds (Rainbow, 36°14′ N Mid-Atlantic Ridge), Abstracts of Papers (Part 2), *32nd Int. Geol. Congr., Florence 2004 (Scientific Session)*, 2004a, p. 1198.

Borodaev, Yu.S., Mozgova, N.N., Gablina, I.F., *et al.*, Zonal Pipes of Black Smokers from the Rainbow Hydrothermal Field (Mid-Atlantic Ridge, 36°14′ N), *Vestn. Mos. Gos. Univ., Ser. 4: Geol.*, 2004b, no. 3, pp. 40–49.

Bortnikov, N.S., Vikentyev, I.V., Appolonov, V.N., *et al.*, The Rainbow Serpentinite-Related Hydrothermal Field, Mid-Atlantic Ridge, 36°14′ N: Mineralogical and Geochemical Features, *Proc. Joint Sixth Meeting. Mineral Deposits at the Beginning of the 21st Century, Krakow, 26–29 August, 2001*, Lisse: Balkema Publ., 2001, pp. 265–268.

Brett, R., Experimental Data from the System Cu–Fe–S and Their Bearing on Exsolution Textures in Ores, *Econ. Geol.*, 1964, vol. 59, pp. 1241–1260.

Cabri, L.J., New Data on Phase Relations in the Cu–Fe–S System, *Econ. Geol.*, 1973, vol. 68, pp. 443–454.

Caye, R., Cervelle, B., Cesbron, F., *et al.*, Isocubanite, a New Definition of the Cubic Polymorph of Cubanite $CuFe_2S_3$, *Miner. Mag.*, 1988, vol. 52, pp. 509–514.

Cherkashev, G., Ashadze, A., Gebruk, A., and Krylova, E., New Fields with Manifestations of Hydrothermal Activity in the Logatchev Area, *InterRidge News*, 2000, vol. 9, no. 2, pp. 26–28.

Chvileva, T.N., Bezsmertnaya, M.S., Spiridonov, E.M., *et al.*, *Spravochnik-opredelitel' rudnykh mineralov v otrazhennom svete* (Reference Book for the Identification of Ore Minerals in Reflected Light), Moscow: Nedra, 1988.

Constantinou, G., Idaite from the Skouriotissa Massive Sulfide Orebody, Cyprus: Its Composition and Conditions of Formation, *Am. Mineral.,* 1975, vol. 60, pp. 1013–1018.

Djurle, C., An X-Ray Study of the System Cu–S, *Chem. Scan*, 1958, vol. 12, no. 7, pp. 1415–1426.

Dubut, J.-L., Lafitte, M., and Maury, J., Stoehiométrie evolutive des pyrites terrestres et oceaniques, in *C.R. Acad. Sci. Ser. II*, Paris, 1982, vol. 295, pp. 587–590.

Eliseev, E.N., Rudenko, L.E., Sinev, L.A., *et al.*, Polymorphism of Copper Sulfides in the Cu_2S–$Cu_{1.8}S$ System, in *Mineralogicheskii sbornik* (Mineralogical Collection), Lvov: Lvov Gos. Univ., 1964, no. 18, pp. 385–400.

Fouquet, Y., Barriga, F., Charlou, J.L., *et al.*, FLORES Diving Cruise with Nautile Near the Azores—First Dives on the Rainbow Field: Hydrothermal Seawater, Mantle Interaction, *InterRidge News*, 1998, vol. 7, no. 1, pp. 24–28.

Gablina, I.F., Mozgova, N.N., Borodaev, Yu.S., *et al.*, Association of Copper Sulfides in Recent Oceanic Ores of the Logatchev Hydrothermal Field (Mid-Atlantic Ridge, 14°45′ N), *Geol. Rudn. Mestorozhd.*, 2000, vol. 42, no. 4, pp. 329–349 [Geol. Ore Dep. (Engl. Transl.), 2000, vol. 42, no. 4, pp. 296–316].

Gablina, I.F., Borodaev, Yu.S., Mozgova, N.N., *et al.*, Tetragonal $Cu_{2-x}S$ in Recent Hydrothermal Ores of the Rainbow Field (Mid-Atlantic Ridge, 36°14′ N), in *Novye dannye o mineralakh* (New Data on Minerals), Moscow: EKOST, 2004, vol. 39, pp. 102–109 (New Data on Minerals, 2004, vol. 39, Ocean Pictures Ltd., pp. 99–105).

Hannington, M.D., Thompson, G., Rona, P.A., and Scott, S.D., Gold and Native Copper in Supergene Sulfides from the Mid-Atlantic Ridge, *Nature*, 1988, no. 333, pp. 64–66.

Krasnov, S., Cherkashev, G., Stepanova, T., *et al.*, Detailed Studies of Hydrothermal Fields in the Atlantic, in *Hydrothermal Vents and Processes*, Parson, L.M., Walker, C.L., and Dixon, D.R., Eds., London: Geol. Soc. Spec. Publ., 1995, vol. 87, pp. 43–64.

Lafitte, M. and Maury, R., Variations de stoechiométrie de chalcopyrites naturelles, *Bull. Mineral.*, 1982, vol. 105, pp. 57–61.

Large, D.J., MacQuaker, J., Vaughan, D.J., *et al.*, Evidence for Low-Temperature Alteration of Sulfides in the Kupferschiefer Copper Deposits of Southwestern Poland, *Econ. Geol.*, 1995, vol. 90, pp. 2143–2155.

Lazareva, L.I., Ashadze, A.M., Batuev, B.N., and Nesterov, A.R., Regularities in the Concentration and Forms of Occurrence of Gold and Silver in Sulfide Ores of the Mir Edifice and Polyarnoe Ore Field in the Mid-Atlantic Ridge, in *Voprosy geokhimii i tipomorfizm mineralov* (Problems of Geochemistry and Typomorphism of Minerals), St. Petersburg: St. Petersb. Gos. Univ., 1998, pp. 93–105.

Lazareva, L., Cherkashov, G., Stepanova, T., and Batuev, B., Rare Minerals in the Rainbow Deposits, *International Conference. Minerals of the Ocean*, St. Petersburg, 20–25 April, 2002, pp. 139–140.

Lein, A.Yu., Ul'yanova, N.V., Ul'yanov, A.A., *et al.*, Mineralogy and Geochemistry of Sulfide Ores in Submarine Hydrothermal Fields Associated with Serpentine Protrusions, *Ross. Zh. Nauk Zemle*, 2001, vol. 3, no. 5, pp. 371–391.

Lein, A.Yu., Cherkashev, G.A., Ul'yanov, A.A., *et al.*, Mineralogy and Geochemistry of Sulfide Ores in the Logatchev-2 and Rainbow Hydrothermal Fields: Similar and Distinctive Features, *Geokhimiya*, 2003, vol. 41, no. 3, pp. 304–328 [*Geochem. Int.* (Engl. Transl.), 2003, vol. 41, no. 3, pp. 271–294].

Lur'e, A.M. and Gablina, I.F., Zonal Sulfide Series in Copper Deposits Associated with Red Rocks, *Geokhimiya*, 1976, vol. 14, no. 1, pp. 109–115.

Merwin, H.E. and Lombard, R.H., The System Cu–Fe–S, *Econ. Geol.*, 1937, vol. 32, pp. 203–284.

Mineraly. Spravochnik (Minerals: Reference Book), Moscow: Akad. Nauk SSSR, 1960, vol. 1, p. 617.

Missack, E., Stoffers, P., and El Goresy, A., Mineralogy, Parageneses, and Phase Relations of Copper-Iron Sulfides in the Atlantis II Deep, Red Sea, *Miner. Deposita*, 1989, vol. 24, pp. 82–91.

Mozgova, N.N., Borodaev, Yu.S., Tsepin, A.I., *et al.*, Nonstoichiometry of Pyrite and Marcasite from Black Smokers (21° S), *Dokl. Akad. Nauk*, 1995a, vol. 343, no. 6, pp. 795–800.

Mozgova, N.N., Nenasheva, S.N., Borodaev, Yu.S., and Tsepin, A.I., Composition Field and Specific Features of Isocubanite Isomorphism, *Geokhimiya*, 1995b, vol. 33, no. 4, pp. 533–552.

Mozgova, N.N., Krasnov, S.G., Batuev, B.N., *et al.*, The First Report of Cobalt Pentlandite from a Mid-Atlantic Ridge Hydrothermal Deposit, *Can. Mineral.*, 1996, vol. 34, pp. 23–28.

Mozgova, N.N., Efimov, A.V., Borodaev, Yu.S., *et al.*, Mineralogy and Chemistry of Massive Sulfides from the Logatchev Hydrothermal Field (14°45′ N Mid-Atlantic Ridge), *Explor. Min. Geol.*, 1999, vol. 8, no. 3/4, pp. 379–395.

Mozgova, N., Borodaev, Yu., Cherkashev, G., *et al.*, High-Temperature Exsolution Structures in Submarine Serpentinite-Related Massive Sulfides (Mid-Atlantic Ridge), *International Conference. Minerals of the Ocean*, St. Petersburg, 20–25 April, 2002a, pp. 134–137.

Mozgova, N.N., Borodaev, Yu.S., Gablina, I.F., *et al.*, Isocubanite from Sulfide Ores of the Rainbow Hydrothermal Field (Mid-Atlantic Ridge, 36°14′ N), *Zap. Vseross. Miner. O-va*, 2002b, no. 5, pp. 61–70.

Mozgova, N.N, Fardust, F., Borodaev, Yu.S., and Trubkin, N.V., Isomorphism and Nonstoichiometry of Pentlandite from Black Smokers in the Rainbow and Logatchev Hydrothermal Fields, *Zap. Vseross. Miner. O-va*, 2005, no. 1, pp. 69–81.

Mumme, W.G., Sparrow, G.J., and Walker, G.S., Roxbyite, a New Copper Sulphide Mineral from the Olympic Dam Deposit, Roxby Downs, South Australia, *Miner. Mag.*, 1988, vol. 52, part 3, pp. 323–330.

Nickel, E.H., Solid Solutions in Mineral Nomenclature, *Can. Mineral.*, 1992, vol. 30, pp. 231–234.

Powell, W.G. and Pattison, D.R.M., An Exsolution Origin for Low-Temperature Sulfides at the Hemlo Gold Deposit, Ontario, Canada, *Econ. Geol.*, 1997, vol. 92, pp. 569–577.

Rajamani, V. and Prewitt, C.T., Crystal Chemistry of Natural Pentlandites, *Can. Mineral.*, 1973, vol. 12, pp. 178–187.

Rambaldi, E.R., Rajan, R.S., Housley, R.M., and Wang, D., Gallium-Bearing Sphalerite in a Metal-Sulfide Nodule of the Qingzhen (EH3) Chondrite, *Meteoritics*, 1986, vol. 21, no. 1, pp. 23–31.

Riley, J.F., The Pentlandite Group (Fe, Ni, Co)$_9$S$_8$: New Data and an Appraisal of Structure-Composition Relationships, *Mineral. Mag.*, 1977, vol. 41, pp. 345–349.

Rona, P.A., Widenfalk, L., and Bostrom, K., Serpentinized Ultramafics and Hydrothermal Activity at the Mid-Atlantic Ridge Crest Near 15° N, *J. Geophys. Res.*, 1987, vol. 92, no. B2, pp. 1417–1427.

Satpaeva, M.K. and Polkanova, E.V., Ferruginous (Anomalous) Bornite in the Dzhezkazgan Ores and Its Extraction from Chalcopyrite, *Tr. Inst. Geol. Nauk K.I. Satpaeva*, 1978, vol. 38, pp. 105–130.

Satpaeva, M.K., Dara, A.D., Kurmakaeva, F.A., and Polkanova, E.V., X-Bornite in the Dzhezkazgan Ores, *Izv. Akad. Nauk Kaz. SSR, Ser. Geol.*, 1974, no. 6, pp. 51–57.

Sillitoe, R.H. and Clark, A.H., Copper and Copper-Iron Sulphides as the Initial Products of Supergene Oxidation, Copiapó Mining District, Northern Chile, *Am. Mineral.*, 1969, vol. 54, pp. 1684–1710.

Simonov, V.A. and Milosnov, A.A., Physicochemical Conditions of Hydrothermal Processes in the Mid-Atlantic Ridge, Fifteen Twenty Fracture Zone, *Geokhimiya*, 1996, vol. 34, no. 8, pp. 760–766 [*Geochem. Int.* (Engl. Transl.), 1996, vol. 34, no. 8, pp. 685–690].

Sugaki, A., Shima, H., Kitakaze, A., and Harada, H., Isothermal Phase Relations in the System Cu–Fe–S under Hydrothermal Conditions at 350°C and 300°C, *Econ. Geol.*, 1975, vol. 70, pp. 806–823.

Torokhov, M.P., Cherkashev, G.A., Stepanova, T.V., and Zhirnov, E.A., Uranium, Its Minerals and Parageneses in Massive Sulphides of the Logatchev-2, MAR Ore Field, *InterRidge News*, 2002, vol. 11, no. 2, pp. 32–33.

Ueno, T., Kitakaze, A., and Sugaki, A., Phase Relations in the $CuFeS_2$-FeS Join, *Tohoku Univ. Sci. Rept.*, 1980, Ser. 3, vol. 16, pp. 283–293.

Vaughan, D. and Craig, J., *Mineral Chemistry of Metal Sulfides*, New York: Cambridge Univ., 1978. Translated under the title *Khimiya sul'fidnykh mineralov*, Moscow, Mir, 1981.

Vikent'ev, I.V., Formation Conditions and Metamorphism of Massive Sulfide Ores, *DSc (Geol.-Miner.) Dissertation*, Moscow: IGEM Ross. Akad. Nauk, 2001.

Vikent'ev, I.V., Bortnikov, N.S., Bogdanov, Yu.A., *et al.*, Mineralogy of Hydrothermal Deposits in the Rainbow Field, the Azores Region (Atlantic), in *Metallogeniya drevnikh i sovremennykh okeanov* (Metallogeny of Ancient and Recent Oceans), Miass: Inst. Miner. Ural. Otd. Ross. Akad. Nauk, 2000, pp. 103–110.

Wintenberger, M., André, G., Garcin, C., *et al.*, Intermediate Valency, Verwey Transition and Magnetic Structures of a New Mineral, $Cu_{1-\varepsilon}Fe_{3+\varepsilon}S_4$, Resulting from the Ageing of Isocubanite, *J. Magnet. Magn. Mater.*, 1994, vol. 132, pp. 31–45.

Yund, R.A. and Kullerud, G., Thermal Stability of Assemblages in the Cu–Fe–S System, *J. Petrol.*, 1966, vol. 7, pp. 454–488.

Zhmodik, S.M., Lisitsyn, A.P., Simonov, V.A., *et al.*, Spatial Distribution of Au in Samples of Oceanic Hydrothermal Sulfide Ores (Logatchev and Broken Spur Fields, MAR), in *Metallogeniya drevnikh i sovremennykh okeanov-2001* (Metallogeny of Ancient and Recent Oceans-2001), Miass: Inst. Miner. Ural. Otd. Ross. Akad. Nauk, 2001, pp. 61–67.